FERMILAB-PUB-77-116-E HPWF-77/1
July 1977

RECEIVED
JUL 14 1977
DIRECTORS OFFICE
FERMILAB

MEASUREMENT OF THE NEUTRAL CURRENT INTERACTIONS OF HIGH ENERGY NEUTRINOS AND ANTINEUTRINOS*

P. Wanderer+, A. Benvenuti,** D. Cline, F. Messing,++ W. T. Ford,*** R. Imlay,
T. Y. Ling, A. K. Mann, D. D. Reeder, C. Rubbia, R. Stefanski, and L. Sulak
Department of Physics, Harvard University, Cambridge, Massachusetts 02138,
and Department of Physics, University of Pennsylvania, Philadelphia, Pennsylvania 19174, and Department of Physics, University of Wisconsin, Madison, Wisconsin 53706, and Fermi National Accelerator Laboratory, Batavia, Illinois 60510

ABSTRACT

Measurements of the ν and $\bar{\nu}$ weak hadronic neutral current total cross sections and hadron energy distributions are consistent with a V-A form for this current. They are three standard deviations from pure V, pure A, or a pure T form and unambiguously exclude V+A and any linear combination of S and P.

Submitted to Physical Review D

* Work supported in part by the U. S. Energy Research and Development Administration and performed at the Fermi National Accelerator Laboratory.

+ Now at Brookhaven National Laboratory, Upton, New York 11973.

** Now at Universita di Bologna, Bologna, Italy.

++ Now at Carnegie-Mellon University, Pittsburgh, Pennsylvania 15213. Submitted in partial fulfillment of the Ph.D. requirements at the University of Pennsylvania.

*** Now at University of Colorado, Boulder, Colorado 80309.

+++ Now at Rutgers University, New Brunswick, New Jersey 08903.

I. INTRODUCTION

The discovery of a class of neutrino interactions which yield no final-state charged lepton was first reported in 1973.[1] Since then, the initial observations of a weak neutral current have been confirmed by subsequent experiments which utilized neutrino and antineutrino beams covering a wide range of energies.[2-13] This paper gives a detailed account of our more recent measurements of neutral current inelastic interactions of high-energy neutrinos and antineutrinos, which were briefly described earlier.[4] The measured ratio of the antineutrino and neutrino neutral current total cross sections $\sigma_N^{\bar{\nu}}/\sigma_N^{\nu}$ and the measured hadron energy distributions are consistent with a V-A form for the neutral current and with the predictions of the gauge theories proposed by Weinberg and Salam[14] and others.[15] The results are three standard deviations from the pure forms V, A, or T, and unambiguously exclude V+A and any linear combination of S and P. In most theories of the weak interaction, the presence of V, A interference implies a parity violating component of the weak neutral current.

In section II we describe the experimental apparatus including the characteristics of the several neutrino and antineutrino beams utilized. Following that we discuss the procedures for event selection (III) and various corrections to the data necessary to obtain $\sigma_N^{\bar{\nu}}/\sigma_N^{\nu}$ (IV). The implications of these results for the space-time structure of the weak neutral current are presented in section V where other recent results are summarized. Conclusions are given in section VI.

II. EXPERIMENTAL APPARATUS

The portion of the apparatus[16] which was used for identifying neutral current interactions is shown in Fig. 1. Neutrinos, incident from the left, interact in a liquid scintillator calorimeter. Muons are identified by their passage through iron absorbers, which filter out hadrons that do not interact in the liquid.

The calorimeter consists of 15 or 16 46-cm-thick modules, with dimensions transverse to the beam of 3.48 m x 7.87 m and a mass of 60 metric tons. The calorimeter measures hadron shower energies E_H with a resolution of ~12% rms for E_H > 20 GeV, and with ~15% rms resolution for lower values of E_H. The measured pion absorption length was 118 cm and the radiation length approximately 65 cm. The calorimeter is approximately an isoscalar target: the ratio of protons to neutrons is 1.32. Optical wide-gap spark chambers (BBC), 2.8 m x 2.8 m in area, are placed after every fourth calorimeter module. These chambers, as well as those used to detect muons (see below), were photographed in two 17.5° stereo views and in a 50° stereo view. In addition to the three views of the spark chambers, the information recorded for each event included the pulse height from each of the calorimeter modules and timing and pulse height information from the scintillation counters.

Two muon detectors were used in the experiment. Detector D1 (Fig. 1) consisted of a 3.6 m x 3.6 m scintillation counter and a 2.8 m x 2.8 m spark chamber placed behind a 35 cm or 70 cm iron shield which absorbed most hadron showers. The counter was segmented with horizontal dividers into three equal-sized portions and the middle section was further segmented into four cells each 40 cm high. Detector D2 was a 2.8 m x 2.8 m spark chamber placed behind a 122 cm thick iron toroid magnet which served as a further hadron shield. This magnet was the first of four used to measure muon momenta in charged current interactions.

Muons traversing D1 or D2 were detected with efficiency >99%. However, muons were not detected if they were produced at too large an angle and thus missed the detector or if they had too low an energy to penetrate the hadron absorbers. Detector D1 had a very high muon acceptance (typically 95%) but a fraction of the events (typically 12%) had hadrons which punched through the hadron absorber and were misidentified as muons. Detector D2 had a lower muon acceptance (typically 84%) but was essentially free of hadron contamination. Tests for possible systematic errors in the discrimination of neutral current (NC) events from charged current (CC) events were made by comparing the two detectors. The characteristics of the two muon detectors are listed in Table I.

Neutrino interactions which produced hadron showers with energy E_H greater than a preset minimum triggered the apparatus. This was the basic trigger for the experiment. The trigger efficiency was 99.5% for E_H > 4 GeV. Counter A was in anticoincidence to prevent triggers from incident charged particles. In order to monitor the E_H trigger, two other triggers were used. One was for muons which were produced by charged current neutrino interactions in the calorimeter and which traversed all four sections of the iron toroidal magnet, and the other was for muons produced in the earth shield upstream of the apparatus. This latter trigger gave a continual calibration of the calorimeter and the optical system. During the time the beam was off, a gate 10% as long as the beam gate was opened in order to measure the background due to cosmic ray showers. This background was measured to be negligible.

We report data taken with four different beams. They were a ν beam produced by 400 GeV protons with a horn focusing system (Horn),[13] ν beams produced by 300 GeV protons (1974 QT) and by 380 GeV protons (1975 QT) with a quadrupole triplet focusing system, and a $\bar{\nu}$ beam produced by 300 GeV protons with a two-horn focusing system and a plug to suppress high-momentum secondaries (DM).

III. EVENT SELECTION

Scanners were instructed to select photographs having at least two related tracks in the second or third spark chamber but no tracks in the first spark chamber (Fig. 1). The tracks in the spark chamber where the shower first appeared were projected back in order to determine the vertex of the interaction. The number of charged particles related to the shower was recorded for each spark chamber. Physicists scanned large portions of all four samples of data. The efficiency of the scanners was found to be 95%, and events missed by the scanners could not be correlated with any variable. The scanning inefficiency was independent of whether or not a muon was present in the muon detectors and independent of the position of the vertex and the hadronic energy of the event (for E_H >4 GeV). In addition, a number of charged-current events were checked by an independent group of scanners. For this check, the transverse coordinates, X and Y, of event vertices were determined from extrapolation of the muon trajectories in the downstream spark chambers. The longitudinal (Z) position of the vertex was determined from the calorimeter pulse heights. The X and Y distributions obtained by the two methods were in good agreement, as shown in Fig. 2. We note also that Fig. 2 does not show a clustering of events about the edges of the detector, as would be expected from certain types of backgrounds (e.g., neutrons incident from the side or neutrino interactions in the earth below and on the side of the calorimeter).

After the visual and electronic information were combined, events were required to have vertices inside the fiducial volume. For the high-statistics 1975 QT data, the fiducial volume was chosen to be ±100 cm in both dimensions transverse to the beam, and calorimeter modules 7 through 11, as shown in Fig. 1. Between two and four hadron absorption lengths were available for measurement of E_H with this Z fiducial region. A correction was applied for energy in the hadron cascade which leaked out from the downstream end of the calorimeter.[16] The fiducial regions for all four data sets are given in Table 1.

The distribution of the number of sparks occurring in the spark chamber where an event was first observed is shown for events with and without muons in Fig. 3. The distributions are very similar in shape. Differences could arise from different distributions in the variable $y = E_H/E_\nu$ for neutral and charged current interactions, since the number of sparks is roughly correlated with E_H, or be due to scanning biases or spark chamber inefficiency. A small difference is expected because each charged current event has an extra track due to the departing muon; hence events with two tracks in the first spark chamber after the vertex were excluded if a muon was seen. This cut removed 3% of the 1975 QT data and 7% of the DH data. However, the cut does depend on E_H and for 4 GeV < E_H <10 GeV 10% of the 1975 QT and 14% of the DH data were eliminated. Errors assigned to data in this E_H interval were increased to take account of the uncertainty due to this cut.

An estimate of the quality of the hadron showers was made for each event selected. Events with large hadron energy had many sparks and well-defined vertices; events with little hadron energy had fewer sparks and less well-determined vertices. It was found, however, that the ratio of neutral current to charged current events did not depend on the estimate of shower quality.

IV. CORRECTIONS TO THE DATA

A. Muon Acceptance Calculation

Because of the choice of the small fiducial volume (~10% of the detector mass) and the large area and high efficiency of the muon identifiers, the acceptance of the apparatus for muons produced in charged current events, ϵ_μ, was near unity. As a consequence, the calculated correction for undetected muons from these events was not particularly sensitive to the details of the neutrino beam spectra or to the detailed nature of the neutrino interaction.

Spectra for three of the neutrino beams are shown in Fig. 4. These spectra were calculated by Monte Carlo techniques based on measurements of π and K production[17] and on the properties of the hadron beam transport and focussing system.[18] The relative ν and $\bar{\nu}$ content of the beams, given by the parameter

$$a = \frac{\text{No. events with } \mu^-}{\text{No. events with } \mu^- + \text{No. events with } \mu^+} \qquad (1)$$

was determined from measurements of charged-current events and reflects the product of the flux and the cross section integrated over the spectrum of the incident beam.

The cross sections for charged-current interactions were measured previously with the same apparatus.[19] In terms of the usual dimensionless scaling variables $x = q^2/ME_H$ and $y = E_H/E_\nu$, with $q^2 = 2\,E_\nu\,E_\mu\,(1-\cos\theta_{\mu\nu})$, the differential cross sections for ν and $\bar{\nu}$ scattering are[20]

$$\text{for } \nu,\ d^2\sigma/dxdy = \frac{G^2ME}{\pi} F_2(x)\ \left[a(x) + b(x)\ (1-y)^2\right] \qquad (2)$$

$$\text{for } \bar{\nu},\ d^2\sigma/dxdy = \frac{G^2ME}{\pi} F_2(x)\ \left[b(x) + a(x)\ (1-y)^2\right] \qquad (3)$$

where $a(x)$ and $b(x)$ can be interpreted as the fractions of quark and antiquark, respectively. Measurements of ν and $\bar{\nu}$ total cross sections near 1 GeV give $\langle b\rangle = \int \bar{q}(x)dx / \int[\bar{q}(x) + q(x)]\,dx = 0.05 \pm 0.02$, where $q(x)$ and $\bar{q}(x)$ are the x-distributions of quarks and antiquarks, respectively.[11] Our data[19] for $E_{\bar{\nu}} < 30$ GeV give 0.05 ± 0.05. In what follows we use the latter value for $E_{\bar{\nu}} < 30$ GeV and for all E_ν, which implies that $\langle a\rangle = 0.95$. We take $F_2(x)$ from our charged current data.[21]

For $E_{\bar{\nu}} > 30$ GeV, where a significant scale breaking effect has been observed,[19] we again use empirically determined values of a and b.[22] The calculation of ϵ_μ is, however, relatively insensitive to this scale breaking effect because the average energy of the DH beam is close to the energy at which the onset of scale breaking takes place, and because in any case ϵ_μ is near unity. To show this, a calculation of ϵ_μ was made using the form of the $\bar{\nu}$ distribution in eq. (3) with $\langle b\rangle = 0.05$ for all $E_{\bar{\nu}}$. This yielded for detector D1 a value of ϵ_μ 0.03 lower than the value $\epsilon_\mu = 0.94$ for the DH run.

The calculation of ϵ_μ takes into account the beam spectra, muon ionization energy loss, resolution in the E_H measurement, and the magnetic field in the iron toroid. The values of ϵ_μ for the 1975 QF data and the DH data are shown as functions of the space coordinates and E_H in Fig. 5. The average values of ϵ_μ for each of the four sets of data are given in Table I.

B. Hadron Punch-Through

Energetic hadrons from neutral current interactions which penetrate the hadron filter will simulate charged current events. For D2, located behind >17

collision lengths of absorber, the punch-through probability ε_p was negligible. The values of ε_p for D1, located behind >5 collision lengths, were ~13% averaged over the detector and the E_μ spectrum for the 1975 QT data. To correct for this misidentification, values of ε_p for D1 were measured using charged-current events which had a muon identified in D2. Correcting for delta-rays,[23] ε_p was the fraction of such events which had more than one particle in D1. Plots of ε_p for the 1975 QT data are shown in Fig. 6, where the attenuation length of the hadron shower is seen to be in agreement with our measured pion absorption length. These values of ε_p, measured for a 70 cm-thick hadron absorber, are consistent with those measured for the 1974 QT and Horn runs, where the hadron absorber was 35 cm thick, when allowance is made for the difference in thickness. The average value of ε_p for each of the four data sets is given in Table I.[26]

For the Horn data, a second procedure was used to check the punch-through correction made by the method discussed above.[13] The difference between the track direction observed in the D1 spark chamber and the direction specified by a line from the event vertex to the position of the track in the D1 spark chamber was determined. From a sample of charged-current events, it was found that, for 93% ± 2% of the muons, the difference of the angles was <100 mr, while only 24% ± 4% of the hadrons had angle differences less than this (Fig. 7). Thus, measurement of the corresponding difference of angles for neutral current event candidates discriminated between muons and hadrons in D1 and allowed hadron punch-through to be removed in a statistical way. This procedure was carried out for cuts at 100 mr and at 60 mr and both gave punch-through corrections that agreed well with those based on ε_p.

Rather than make a large correction for hadron punch-through for events with E_μ >100 GeV, such events were excluded from the 1975 QT data. The determination of the neutral current to charged current cross section ratio is nearly insensitive to this cut because the events with E_μ > 100 GeV were only 10% of the data and because they had approximately the same neutral current to charged current ratio as events with lower E_μ. For similar reasons, events from the 1974 QT run with E_μ >40 GeV (25% of the total) were excluded. The Horn and DH runs, with lower beam energies, were not affected by this cut.

C. Corrections and Checks

The observed ratio of neutral current to charged events,

$$R_{raw} = \frac{\text{number of events with no detected muon}}{\text{number of events with a detected muon}} \qquad (4)$$

was corrected for the effects of muon acceptance and hadron punch-through with the formula

$$R = \frac{(\varepsilon_\mu + \varepsilon_a - \varepsilon_\mu\varepsilon_a)(1 + R_{raw}) - 1}{1-\varepsilon_p(1 + R_{raw})} \quad . \qquad (5)$$

R_{raw} shows significant variation with vertex location due to changes in muon acceptance and hadron punch-through as exhibited in the largest sample, the 1975 QT data, shown in Fig. 8a and 9a. After correction, R is approximately constant as a function of vertex position and is the same for both detectors (Fig. 8b and 9b). Similar plots for the other three data sets also show R to be constant as a function of vertex position; the DH data are shown in Fig. 10. The uniformity of R versus vertex position is strong evidence that the corrections have been applied correctly and that no serious contamination is present in the neutral current sample.

The values of R determined from eq. (5) are relatively insensitive to errors in ϵ_μ and ϵ_p. For example, the 1975 QT data had $\langle\epsilon_p\rangle = 0.12$, $\langle\epsilon_\mu\rangle = 0.95$. If the punch-through ϵ_p or the fraction of muons which are missed, $1 - \epsilon_\mu$, are changed by 25% (i.e., $\langle\epsilon_p\rangle = 0.15$, $\langle\epsilon_\mu\rangle = 0.94$), the value of R, 0.30, changes by 6% (±0.02).

A further independent check on the corrections is made by comparing the calculated and measured E_μ distributions of events with visible muons in Fig. 11, where the data are seen to be consistent with the calculation.

D. Background due to ν_e Interactions

The interactions of electron-type neutrinos simulate neutral current events in our apparatus. The ν_e contamination of the ν_μ spectrum was calculated the same way as the ν_μ spectrum. The background due to ν_e interactions is negligible for measurements of the total cross section. A 3% correction was made to the distributions in E_μ at the highest values of E_μ.[18]

V. EXPERIMENTAL RESULTS

The data can be used to determine the space-time structure of the weak neutral current in two ways. First, we obtain the total cross section ratio for neutral currents, $\sigma_N^{\bar\nu}/\sigma_N^{\nu}$, from the measured values of R for ν and $\bar\nu$. This cross section ratio will be unity if the neutral current has one of the pure forms, V, A or T, or is any linear combination of S and P, since then no interference terms that change sign under the interchange of neutrino and antineutrino are present in the expressions for the ν and $\bar\nu$ cross sections. If different than unity, the cross section ratio can be used to determine the mixture of currents present. Second the inelasticity ($y \equiv E_H/E_\nu$) distribution for neutral current interactions is related to the directly measured distribution in E_H. In the quark parton model, the y-distributions for any combination of V and A currents will have the forms[25]

$$\frac{1}{E}\frac{d\sigma_N^{\nu}}{dy} = \text{const.}\ \left[a + b(1-y)^2\right],\quad \frac{1}{E}\frac{d\sigma_N^{\bar\nu}}{dy} = \text{const.}\ \left[b + a(1-y)^2\right] \qquad (6)$$

where E is the neutrino energy and a and b are the relative fractions of quarks and (non-strange) antiquarks, respectively (a+b=1). The y-distribution for any mixture of V and A currents can be duplicated by some combination of S, P and T interactions. Nonetheless, specific combinations of S, P and T interactions can be tested. The y-distribution for any mixture of S and P currents is the same for ν and $\bar\nu$:

$$\frac{1}{E}\frac{d\sigma}{dy} = \text{const.}\ y^2 \quad . \qquad (7)$$

For a pure T neutral current, the y-distribution is also identical for ν and $\bar\nu$:

$$\frac{1}{E}\frac{d\sigma}{dy} = \text{const.}\ (1-\tfrac{1}{2}y)^2 \quad . \qquad (8)$$

Interference terms between T and S,P currents will have the form y (2-y).

A. Total Cross Sections

The ratio R_{raw} for each data set was corrected for hadron punch-through and muon acceptance to yield

$$R = \sigma_N(E_H > 4\ \text{GeV})/\sigma_C(E_H > 4\ \text{GeV}) \quad . \tag{9}$$

The corrected ratio R is related to the neutral current to charged current ratios for ν and $\bar{\nu}$, R^{ν} and $R^{\bar{\nu}}$, by the parameter α (eq. 1), which gives the $\nu(\bar{\nu})$ contamination of the $\bar{\nu}(\nu)$ beams:

$$R = \alpha R^{\nu} + (1-\alpha)R^{\bar{\nu}} \quad . \tag{10}$$

The values of R^{ν} and $R^{\bar{\nu}}$ determined from the four samples of data are given in Table II.

Previously, we reported[7] the values $R^{\nu} = 0.11 \pm 0.05$ and $R^{\bar{\nu}} = 0.32 \pm 0.09$, both for $E_H > 4$ GeV. The difference between the earlier value of R^{ν} and the values given in Table II is due to the difficulty of the method used to extract R^{ν} and $R^{\bar{\nu}}$ from the first data samples. We believe that these systematic errors have been appreciably reduced in the samples of data in Table II which are also statistically more significant and were taken with beams of higher purity of ν or $\bar{\nu}$.

Generally, it is not possible to obtain the ratio of the total cross sections $\sigma_N^{\bar{\nu}}/\sigma_N^{\nu}$ from $\sigma_N^{\bar{\nu}}(E_H > 4)/\sigma_N^{\nu}(E_H > 4)$ in a way that is independent of a model of the space-time structure of the neutral current. However, model-independent limits on $\sigma_N^{\bar{\nu}}/\sigma_N^{\nu}$ can be obtained. If the neutral current has exactly the same space-time structure as the charged current, the ratios R^{ν} and $R^{\bar{\nu}}$ will not depend on the cut $E_H > 4$, since the y-distributions for both neutral and charged current interactions are the same.[26] The inequality $R^{\nu}(E_H > 0) \geq R^{\nu}(E_H > 4)$ will obtain for any V,A combination for the neutral current if the charged current is close to V-A. This result is a consequence of the fact that the distribution dN/dy is constant in y for V-A. Admixing the form V+A introduces a $(1-y)^2$ component to the neutrino distribution, and forces proportionately more events to have lower E_H. Similarly, $R^{\bar{\nu}}(E_H > 0) < R^{\bar{\nu}}(E_H > 4)$. The antiquark content of roughly 52 does not change the inequality.

The ratio $\sigma_N^{\bar{\nu}}/\sigma_N^{\nu}$ may be calculated from R^{ν}, $R^{\bar{\nu}}$ (for $E_H > 0$) and the measured ratio of the charged current cross sections for neutrinos and antineutrinos with the relation: $\sigma_N^{\bar{\nu}}/\sigma_N^{\nu} = (R^{\bar{\nu}}/R^{\nu})(\sigma_C^{\bar{\nu}}/\sigma_C^{\nu})$. Since the ratio of the charged-current cross sections is changing with energy,[19] it is necessary to specify the energy at which the calculation is made. Noting from Table II that R^{ν} is approximately constant over the average energy interval from 53 GeV to 83 GeV, and that it is the same as that obtained by the Gargamelle experiment[11] for $E_{\nu} \sim 1$ GeV, we take that same value of R^{ν} at 41 GeV, the average energy of the DM beam used to obtain $R^{\bar{\nu}}$. At 41 GeV we calculate the inequality

$$\frac{\sigma_N^{\bar{\nu}}}{\sigma_N^{\nu}} \leq \frac{R^{\bar{\nu}}}{R^{\nu}} \cdot \frac{\sigma_C^{\bar{\nu}}}{\sigma_C^{\nu}} = \left(\frac{0.39 \pm 0.10}{0.29 \pm 0.04}\right)(0.45 \pm 0.08)$$

$$\frac{\sigma_N^{\bar{\nu}}}{\sigma_N^{\nu}} \leq 0.61 \pm 0.25 \tag{11}$$

where the ratio $\sigma_C^{\bar{\nu}}/\sigma_C^{\nu}$ is obtained from earlier measurement.[19]

To obtain $\sigma_N^{\bar{\nu}}/\sigma_N^{\nu}$, rather than its upper limit, it is necessary to correct for events with $E_H < 4$ GeV. We test possible forms for the weak neutral current by using the assumed form to correct the data for missing events and then comparing the values for $\sigma_N^{\bar{\nu}}/\sigma_N^{\nu}$ so obtained with the values expected for that form. Because of the high energy of the neutrino beams, the fraction of neutrino events with $E_H < 4$ GeV is small (~7%). Thus, for any combination of V and A

currents (any value of the coefficient a in Eq. 6), the difference between $R^{\nu}(E_H > 0)$ and the measured value, $R^{\nu}(E_H > 4)$, is negligible within experimental error. The ratio $R^{\bar{\nu}}$ is more sensitive to the exact form of the interaction because the average antineutrino beam energy is lower. For various forms of the weak neutral current given in Table III, the corrected, experimental values of $\sigma_H^{\bar{\nu}}/\sigma_H^{\nu}$ are compared with the expected values for this ratio. From Table III, S,P and (V+A) forms are clearly ruled out. The experimental value of $\sigma_H^{\bar{\nu}}/\sigma_H^{\nu}$ for pure V, A or T is 3 standard deviations away from the expected value but is within 1 standard deviation of the value expected for V-A.

We obtain the best fit for the space-time structure of the neutral current by using the general forms of the $y \equiv E_H/E_\nu$ distribution given in Eq. (6). For a V-A interaction, $a \approx 1$ and $b \approx 0$, while pure V or pure A require $a = b = \frac{1}{2}$. The best fit is obtained by varying a and b until the expected value of $\sigma_H^{\bar{\nu}}/\sigma_H^{\nu}$ agrees with the corrected experimental value. For the best fit, $\sigma_H^{\bar{\nu}}/\sigma_H^{\nu} = 0.46 \pm 0.20$, $a = 0.85 \pm 0.12$, $b = 0.15 \pm 0.12$. This gives the equivalent forms for the weak neutral current: $A - (0.7 \pm 0.3)\ V$ or $V - (0.7 \pm 0.3)\ A$.[27] The total cross section ratios are then $R^{\nu}(E_H>0) \equiv \sigma_N^{\nu}/\sigma_C^{\nu} = 0.30 \pm 0.04$, $R^{\bar{\nu}}(E_H>0) \equiv \sigma_N^{\bar{\nu}}/\sigma_C^{\bar{\nu}} = 0.33 \pm 0.05$.[28]

More generally, the effective Lagrangian for neutral current interactions may be written in the quark-parton model as[29]

$$\mathcal{L} = \frac{G}{\sqrt{2}}\,\bar{\nu}\gamma_\lambda\,(1+\gamma_5)\nu\,\Big\{\tfrac{1}{2}\big[\bar{u}\gamma_\lambda\,(V_3 + A_3\gamma_5)u - \bar{d}\gamma_\lambda\,(V_3 + A_3\gamma_5)d\big] + \tfrac{1}{2}\big[\bar{u}\gamma_\lambda\,(V_1 + A_1\gamma_5)u + \bar{d}\gamma_\lambda\,(V_1 + A_1\gamma_5)d\big]\Big\} \tag{12}$$

where V_3, A_3, V_1 and A_1 are, respectively, the coupling constants of isovector-vector, isovector-axial vector, isoscalar-vector and isoscalar-axial vector currents, and the interactions of $s\bar{s}$ etc. quarks are neglected. In this notation, the overall strength of the weak hadronic neutral current relative to the charged current is:

$$\sigma_+ \equiv \frac{\sigma_N^{\nu} + \sigma_N^{\bar{\nu}}}{\sigma_C^{\nu} + \sigma_C^{\bar{\nu}}} = \tfrac{1}{2}(V_3^2 + A_3^2 + V_1^2 + A_1^2) = 0.30 \pm 0.05\ . \tag{13}$$

Further, the vector-axial vector interference is measured by

$$\sigma_- \equiv \frac{\sigma_N^{\nu} - \sigma_N^{\bar{\nu}}}{\sigma_C^{\nu} - \sigma_C^{\bar{\nu}}} = \tfrac{1}{2}(V_3A_3 + V_1A_1) = 0.26 \pm 0.14\ . \tag{14}$$

The ratio $\frac{\sigma_-}{\sigma_+} = 0.87 \pm 0.35$, where we expect +1 for V-A or A-V interference, 0 for pure V or pure A, and -1 for V+A interference.

The inequality of σ_N^{ν} and $\sigma_N^{\bar{\nu}}$ requires the presence of both V and A components in the interaction. In the conventional model, where the interaction is carried by a single W^0, this requires that the weak neutral current be parity violating. It is possible, nonetheless, to construct models of the neutral current which would contain both V and A currents and V,A interference terms and still be parity-conserving.[30] Direct observation of parity violation in ν interactions requires measurement of a nonzero pseudoscalar quantity which has not been accomplished as yet in either charged or neutral current ν interactions. Direct observation of parity violation is in principle possible in the atomic physics experiments which measure the scattering of polarized light by heavy atoms, although to date those experiments exhibit a null effect.[31]

The results of the experiment described here have been confirmed by other recent measurements.[6,11] Our measurements of σ_N/σ_C for ν and $\bar{\nu}$ are compared with those of the Gargamelle experiment[11] in Fig. 12. Within errors, the ratios are constant, implying an approximately linear rise of σ_N^{ν} and $\sigma_N^{\bar{\nu}}$ with energy and a diagonal form for the neutral current.[32] The overall

relative strength of the neutral current obtained in Eq. (13), 0.30 ± 0.05, is in good agreement with the value obtained in the CalTech-Fermilab experiment,[6] 0.30 ± 0.065.

B. Distribution in Hadron Energy

The structure of the neutral current can be determined by comparing the measured distribution $d\sigma_N/dE_H$ with that expected for different forms of the neutral current. This determination is independent of the charged-current cross sections, since the uncertainty in the calculation of the muon detection efficiency ϵ_μ is small. It is also independent of the behavior of the neutral current cross section for E_H <4 GeV.

The measured distributions dN/dE_H for the 1975 Quadrupole Triplet ν data and for the Double Horn $\bar{\nu}$ data are compared with several possible forms for these distributions in Figs. 13 and 14. The calculated distributions were obtained by folding the y-distribution with the spectra shown in Fig. 4, for the appropriate mixture of ν and $\bar{\nu}$ (Fig. 15). For the 1975 QT data, the distributions calculated for S and P mixtures, for T interference with S and P, and for V+A currents are much different in shape than the measured distributions. Both V-A and pure V or pure A forms are consistent with the measured distributions. As with V-A, $d\sigma/dy$ for a pure T neutral current falls with increasing y; consequently, it is not excluded by the E_H data. The comparisons made in Figs. 13 and 14 give a neutral current structure that is consistent with the structure obtained from the ratio $\sigma_N^{\bar{\nu}}/\sigma_N^{\nu}$. We have not fitted a form for the neutral current to the E_H distributions for the 1975 Quadrupole Triplet data and the Double Horn data simultaneously because the relative normalization of the ν and $\bar{\nu}$ fluxes is poorly known.

C. Model Comparisons

The ratios R^{ν} and $R^{\bar{\nu}}$ are compared with the predictions of the Weinberg-Salam model in Fig. 16. Each ratio $R^{\nu}(E_H > 0) = \sigma_N^{\nu}/\sigma_C^{\nu}$ and $R^{\bar{\nu}}(E_H > 0) = \sigma_N^{\bar{\nu}}/\sigma_C^{\bar{\nu}}$ independently determines a value for $\sin^2\theta_W$. From Fig. 16, R^{ν} gives $\sin^2\theta_W$ = 0.23 ± 0.06. A similar value of $\sin^2\theta_W$ is obtained from $R^{\bar{\nu}}$. In Fig. 17, the data are compared with the Weinberg-Salam theory in a way that is independent of the coupling constant of the neutral current.

VI. CONCLUSIONS

From measurements of neutrino and antineutrino deep inelastic scattering, we have determined the overall strength of the weak hadronic neutral current relative to the charged current to be (0.30 ± 0.05). The space-time structure of the neutral current is best fitted by the form V-(0.7 ± 0.3)A. Our results are also consistent with a V-A form for the neutral current, but are inconsistent with V+A, combinations of S and P, or with the presence of strong interference terms between S, P and T. At the level of 3 standard deviations, they discriminate against pure V, A, or T forms. For present conventional theories of the weak interaction, these experimental results require a significant parity violating component of the weak neutral current. The corrected ratios of total cross sections are:

$$R^{\nu}(E_H > 0) \equiv \sigma_N^{\nu}/\sigma_C^{\nu} = 0.30 \pm 0.06$$

$$R^{\bar{\nu}}(E_H > 0) \equiv \sigma_N^{\bar{\nu}}/\sigma_C^{\bar{\nu}} = 0.33 \pm 0.09 \ .$$

Together with the results of other neutrino experiments, the data described here are consistent with a linear dependence of $\sigma_N^{\bar{\nu}}$ and σ_N^{ν} on neutrino energy. In the context of the Weinberg-Salam gauge theory, these data yield $\sin^2\theta_W$ = 0.23 ± 0.06.

The V, A structure of the weak neutral current obtained here is consistent with the implications of measurements of the electric dipole moments of certain atoms and molecules, which limit the strength of S, P, or T couplings to 10^{-3} G,[33] and also with calculations of stellar evolution rates, which limit the strength of a tensor current T to <0.02 G.[34]

We are grateful for the conscientious scanning of W. Grant, A. Black, and P. Oehlig, for the technical work of R. Beck, E. Mayer, L. Thomas, and M. Wredon, for the engineering of the Physical Sciences Laboratory of the University of Wisconsin, and for the continuing assistance and encouragement of the Fermilab staff. We thank Z. Paschos for useful discussions. One of us (F.W.) thanks Brookhaven National Laboratory for support during the final phase of this work.

FOOTNOTES AND REFERENCES

1. C. Hyett, in Proc. Sixth Intnl. Symposium on Electron and Photon Interactions at High Energies, Bonn, 1973, ed. by H. Rollnik and W. Pfeil (North-Holland, Amsterdam, 1974), p. 389; F. J. Hasert et al., Phys. Lett. 46B, 138 (1973); A. Benvenuti et al., Phys. Rev. Lett. 32, 800 (1974); F. J. Hasert et al., Nucl. Phys. B73, 1 (1974).
2. B. Aubert et al., Phys. Rev. Lett. 32, 1454 (1974).
3. A. Benvenuti et al., Phys. Rev. Lett. 32, 1457 (1974).
4. A. Benvenuti et al., Phys. Rev. Lett. 37, 1039 (1976).
5. D. C. Barish et al., Phys. Rev. Lett. 34, 538 (1975).
6. B. C. Barish et al., Proc. XVIII Conf. on High Energy Physics, Tbilisi, USSR, 1976, ed. by N. N. Bogoliubov et al. (Joint Institute for Nuclear Research, Dubna, 1977), p. B109.
7. F. Schreiner, Neutrinos '76 Conference, Aachen, Germany, June 8-12, 1976; S. J. Barish et al., Phys. Rev. Lett. 33, 448 (1974).
8. D. Cline et al., Phys. Rev. Lett. 37, 252, 648 (1976).
9. W. Lee et al., Phys. Rev. Lett. 37, 186 (1976).
10. J. Blietschau et al., Nucl. Phys. B114, 189 (1976).
11. J. Blietschau et al., Nucl. Phys. B118, 218 (1977).
12. F. Reines, H. S. Gurr, and H. W. Sobel, Phys. Rev. Lett. 37, 315 (1976).
13. F. Messing, "A Search for Weak Neutral Currents in Semileptonic Interactions," thesis, University of Pennsylvania, 1975 (unpublished).
14. S. Weinberg, Phys. Rev. Lett. 19, 1264 (1967) and 27, 1688 (1972); Phys. Rev. D5, 1412 (1972); A. Salam and J. C. Ward, Phys. Lett. 13, 168 (1964). See also A. Pais and S. B. Treiman, Phys. Rev. D6, 2700 (1972).
15. F. Gürsey and P. Sikivie, Phys. Rev. Lett. 36, 775 (1976).
16. A. Benvenuti et al., Nucl. Instrum. Methods 125, 447, 457 (1975).

17. B. Aubert et al., Colloque Internationaux du CNRS, La Physique Du Neutrino a Haute Energie, Paris, 1975, ed. by A. Rousset and P. Petiau (Editions du Centre National De La Recherre Scientifique, Paris), p. 385; A. Benvenuti et al., Ibid. p. 397.

18. R. J. Stefanski and H. B. White, "Neutrino Flux Distributions," Fermilab report 5M 292, 1976 (unpublished).

19. B. Aubert et al., Phys. Rev. Lett. 33, 984 (1974); A. Benvenuti et al., Phys. Rev. Lett. 36, 1478 (1976).

20. J. D. Bjorken and E. A. Paschos, Phys. Rev. D1, 3151 (1970).

21. A fit to the data gave $F_2(x) = 0.55\,(1-x^2)^5 + 0.38\,x^{0.6}\,(1-x^2)^3$.

22. The charged-current cross sections were $\frac{d^2\sigma_C^\nu}{dxdy} \propto F_2(x)\,(b(x) + a(x)\,(1-y)^2)$ where $a(x) + b(x) = 1$ and $a(x) = 0.95$ for $E_{\bar\nu} < 30$ GeV

$a(x) = 0.52$ for 30 GeV $< E_{\bar\nu} <$ 50 GeV, $x < 0.15$

$a(x) = 0.95$ for 30 GeV $< E_{\bar\nu} <$ 50 GeV, $x > 0.15$

$a(x) = 0.40$ for 50 GeV $< E_{\bar\nu}$, $x < 0.15$

$a(x) = 0.90$ for 50 GeV $< E_{\bar\nu}$, $x > 0.15$.

23. The probability that a muon would be accompanied by a delta ray was established to be 0.14 ± 0.014 from a scan of muons passing through D2 and the spark chambers further downstream.

24. The measured values of ϵ_p are expected to be slightly lower than the actual values due to the granularity of the liquid scintillator container. However, since the spark chamber covered the central 80% of the counter area, the effect of this granularity is quite small.

25. R. L. Kingsley, F. Wilczek, A. Zee, Phys. Rev. D10, 2216 (1974); B. Kayser, C. T. Carvey, Z. Fishbach, S. P. Rosen, Phys. Lett. 52B, 385 (1974); S. Pakvasa, G. Rajasekaran, Phys. Rev. D12, 113 (1975); J. J. Sakurai, Neutrinos - 1974, Philadelphia, 1974, ed. by C. Baltay (American Institute of Physics, New York), p. 57.

26. We neglect the production of single strange particles by the charged current, which is <5% of the total charged current cross sections.

27. We have neglected isoscalar contributions which are not V-A.

28. If the value of $\sigma_C^{\bar\nu}/\sigma_C^{\nu}$ were taken as 0.38, the corresponding values of $\sigma_N^{\bar\nu}/\sigma_N^{\nu}$ and $R^{\bar\nu}(E_H < 0)$ are 0.44 and 0.35, respectively.

29. J. J. Sakurai, "Phenomenology of Neutral Current Interactions," preprint UCLA/76/TEP/21, 1976; E. A. Paschos, Proc. 10th Recontre de Moriond, Moriond, 1975, ed. J. Tran Thanh Van (Laboratoire de Physique Theorique et Particules Elementaires, Orsay), p. 261.

30. T. H. Fritzsch and P. Minkowski, Nucl. Phys. B103, 61 (1976); L. Wolfenstein in Proc. Intnl. Symposium on Lepton and Photon Interactions at High Energy, op. cit., p. 613; B. Kayser, Phys. Rev. D (to be published); R. N. Mohapatra and D. P. Sidhu, Phys. Rev. Lett. 38, 667 (1977).

31. P.E.G. Baird et al., Nature 264, 528 (1976).

32. E. A. Paschos, Phys. Rev. D15, 1966 (1977); S. L. Glashow and S. Weinberg, Phys. Rev. D15, 1958 (1977).

33. E. H. Hinds, C. E. Loving, and P.G.H. Sandars, Phys. Lett. 62B, 97 (1976).

34. P. Sutherland et al., Phys. Rev. D13, 2700 (1976).

Table I. Relevant parameters for the four experiments reported here. The numbers of events have been corrected for muon detection efficiency and hadron punch-through. The parameter α, obtained from the measured CC events, indicates the composition of the beams.

Beam Type	$\alpha = \frac{N_{\mu^-}}{N_{\mu^-} + N_{\mu^+}}$	Number of Events		Muon Detection Efficiency ϵ_μ		Hadron Filter Thickness (cm)	Hadron Punch-Through Probability ϵ_p		Fiducial Volume	
		Neutral	Charged	Det. D1	Det. D2		Det. D1	Det. D2	Maximum $\lvert X\rvert, \lvert Y\rvert$ (cm)	Z range (modules)
Horn	0.94	266	857	0.83	*	35	0.24	∿ 0	120	5 - 12
1974 QT	0.83	158	599	0.84	*	35	0.20	∿ 0	120	5 - 12
1975 QT	0.86	300	1042	0.95	0.84	70	0.12	∿ 0	100	7 - 11
DII	0.27	69	198	0.94	0.79	70	0.07	∿ 0	100	9 - 11

* Detector 2 had a different geometry for these experiments.

Table II. The values of R^{ν} or $R^{\bar{\nu}}$ for $E_H > 4$ GeV. The errors assigned to R^{ν} and $R^{\bar{\nu}}$ include both statistical and systematic effects, with the predominant contribution being the statistical uncertainty.

Beam type	$R^{\nu}(E_H > 4)$	$R^{\bar{\nu}}(E_H > 4)$	Comment
Mono	0.31 ± 0.06		Pure ν beam, $\langle E_\nu \rangle$ = 53 GeV
1974 QT	0.24 ± 0.06		Mixed beam $\langle E_\nu \rangle$ = 78 GeV
1975 QT	0.29 ± 0.04		Mixed beam $\langle E_\nu \rangle$ = 85 GeV
DBI		0.39 ± 0.10	Pure $\bar{\nu}$ beam $\langle E_{\bar{\nu}} \rangle$ = 41 GeV

Table III. The measured values of $\sigma_H^{\bar{\nu}}/\sigma_H^{\nu}$, after correction for the loss of events with $E_H < 4$ GeV according to the form of the weak neutral current in the first column. The corresponding values of $\sigma_H^{\bar{\nu}}/\sigma_H^{\nu}$, expected from theory, are given in column three. An antiquark contribution of 5% has been assumed.

Form of the weak neutral current	$\sigma_H^{\bar{\nu}}/\sigma_H^{\nu}$	
	Corrected experimental value	Expected value
V - A	0.61 ± 0.25	0.38
V or A	0.40 ± 0.17	1.00
V+A	0.37 ± 0.16	2.65
S or P or S,P mixture	0.26 ± 0.09	1.00
S,P interference with T	0.31 ± 0.11	1.00
T	0.45 ± 0.15	1.00

FIGURE CAPTIONS

Fig. 1 (a) Schematic view of that portion of the target-detector used to identify neutral current and charged current neutrino interactions. Not shown are the remaining three sections of iron toroidal magnet. (b) Display of the calorimeter and spark chamber information for a neutral current event. The side view of the wide gap spark chambers (WGSC) is from one of the 15° stereo views; the top view of the WGSC is from the 90° stereo view. The pulse heights in the calorimeter modules illustrate the development and absorption of the hadron shower, which had E_H = 16.5 GeV. (The gaps in the pulse height distribution show the location of the WGSC.) No particles appear in D1 behind the hadron absorber.

Fig. 2 The X and Y distributions of shower vertices as determined by the two methods discussed in the text. The distributions reflect the 4-cm radius of the ν beam and the position of the detector with respect to the beam.

Fig. 3 Distribution of the number of sparks for neutral current (NC) and charged current (CC) events for two data sets, for events with E_H > 4 GeV. The vertical scales, which are different for NC and CC events, have been chosen so that the NC and CC histograms have equal areas.

Fig. 4 Neutrino spectra for three of the beams used in the experiment. The spectrum of the 1974 QT beam is similar in shape to that of the 1975 QT beam but with lower average neutrino energy because the proton energy was 300 GeV.

Fig. 5 Plots of the muon detection efficiency, ϵ_μ, for the 1975 QT data [(a) – (c)] and the DM data [(d) – (f)] as functions of hadron energy E_H and the longitudinal and transverse positions of the interaction. In plotting the transverse position, the data are classified by defining a series of "square annuli" which cover the detector from the center out to 120 cm. Each "square annulus" is the region defined by the square $|X| < \ell_2$, $|Y| < \ell_2$, $|X| < \ell_1$, $|Y| < \ell_1$, where $\ell_2 - \ell_1$ = 20 cm, with ℓ_2 in 20 cm steps. In each figure, arrows indicate the fiducial region.

Fig. 6 The probability that hadrons will be observed in D1 and in the WGSC spark chamber, ϵ_p, is plotted versus (a) E_H and (b) Z (calorimeter module). The straight line illustrates a pion attenuation length of 118 cm.

Fig. 7 Measured angular errors in the Y-Z plane ($\Delta\theta_y$) and in the X-Z plane ($\Delta\theta_x$) for (a) muon tracks and (b) hadron tracks measured in the D1 spark chamber.

Fig. 8 The ratios of neutral current events to charged current events for the 1975 QT data (a) R_{raw} and (b) R, as defined in the text, are plotted against longitudinal position (calorimeter module number).

Fig. 9 The ratios of neutral current events to charged current events for the 1975 QT data (a) R_{raw} and (b) R, as defined in the text, are plotted against transverse position ("region" is defined in Fig. 5).

Fig. 10 The corrected ratio of neutral current events to charged current events R, defined in the text, is plotted against (a) transverse position and (b) longitudinal position for the DM data.

Fig. 11 Comparison between the calculated and measured hadron energy distributions for charged current events for (a) the 1975 QT data and (b) the DH data. The calculation, shown by the solid line, has been normalized to give the number of events in the histogram.

Fig. 12 The ratio of the total neutral current cross section to the total charged current cross section for (a) neutrinos and (b) antineutrinos is shown as a function of average beam energy for this experiment and for the Gargamelle experiment (ref. 11). The total cross sections include contributions from events with low hadron energy which are not detected in the experiments. These contributions are obtained by calculation as discussed in the text.

Fig. 13 The measured hadron energy distributions for neutral current events are compared with those expected for neutral currents which are S, pure T, which are S, P admixtures and which contain T-S, P interference terms, (a) for the largely ν 1975 QT run and (b) for the largely $\bar{\nu}$ DH run. The calculated distributions have been normalized to the measured number of events.

Fig. 14 The measured hadron energy distributions of neutral current events are compared with those expected for neutral currents which are pure V or pure A, V-A, or V+A in form, (a) for the largely ν 1975 QT run and (b) for the largely $\bar{\nu}$ DH run. The calculated distributions have been normalized to the measured number of events.

Fig. 15 The parameter α, which gives the ν content of the mixed beams, is plotted against hadron energy E_H for two of the runs. The acceptance cutoff in E_H is also shown. For the 1975 QT beam, the average value of α is 0.86. For the DH beam, where the flux falls rapidly for E_ν >10 GeV, $\langle\alpha\rangle$ = 0.27.

Fig. 16 The ratios of the neutral current to charged current cross sections of ν and $\bar{\nu}$ as determined in this experiment and in the Gargamelle experiment (ref. 11) are compared with the Weinberg-Salam theory. The results of this experiment are to be compared with the solid line, which takes into account the rise in $\sigma_c^{\bar{\nu}}/\sigma_c^{\nu}$ with energy. The results of the Gargamelle experiment are to be compared to the dashed curve, where $\sigma_c^{\bar{\nu}}/\sigma_c^{\nu}$ is constant with energy. The numbers along the curves indicate values of $\sin^2\theta_w$.

Fig. 17 The ratio $\sigma_N^{\bar{\nu}}/\sigma_N^{\nu}$ and its error are indicated by the central horizontal line and the cross-hatched area. The datum is compared with the value expected if the neutral current has a pure V, A, S, P, T form and with the prediction of the Weinberg-Salam model.

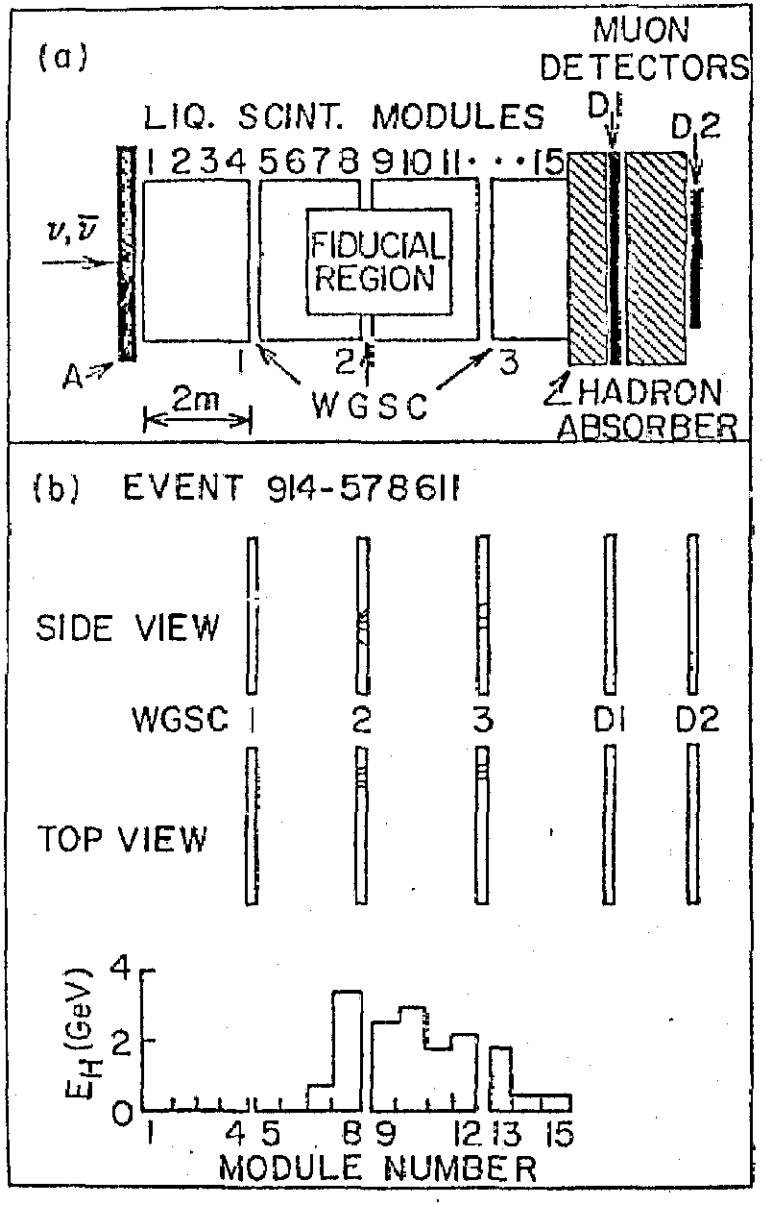

FIGURE 1

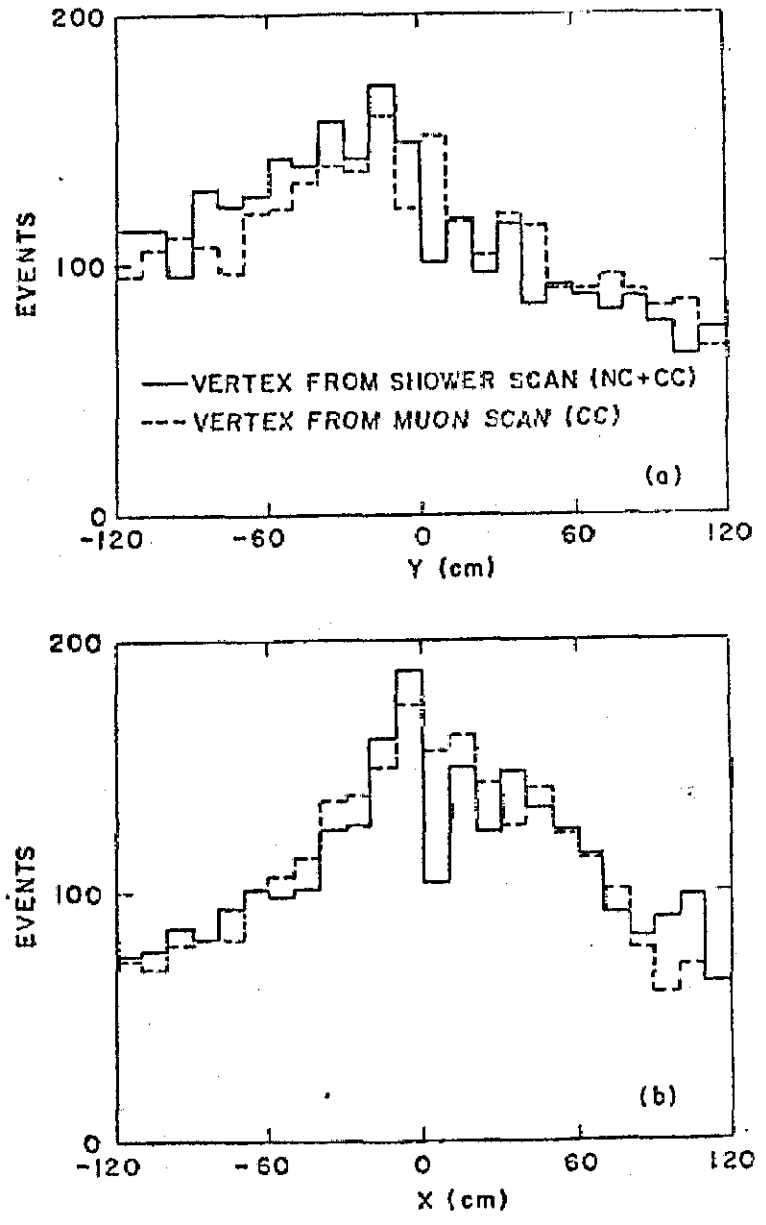

FIGURE 2

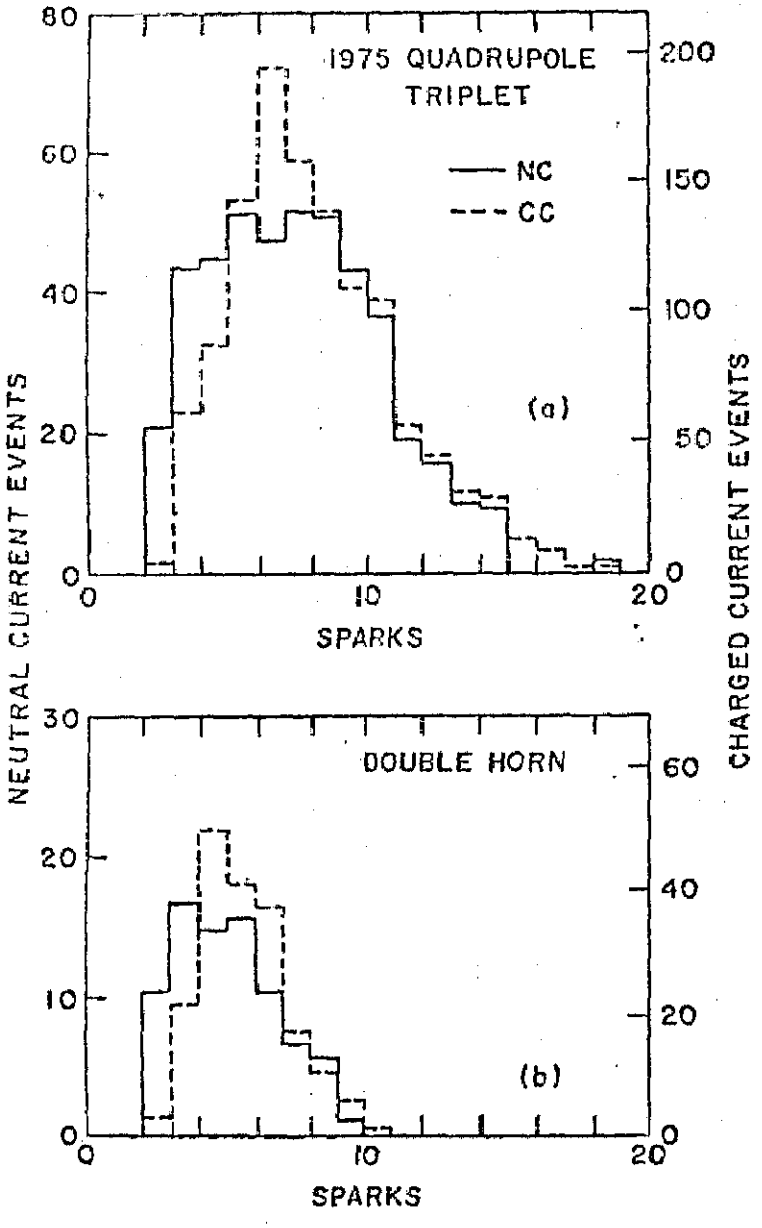

FIGURE 3

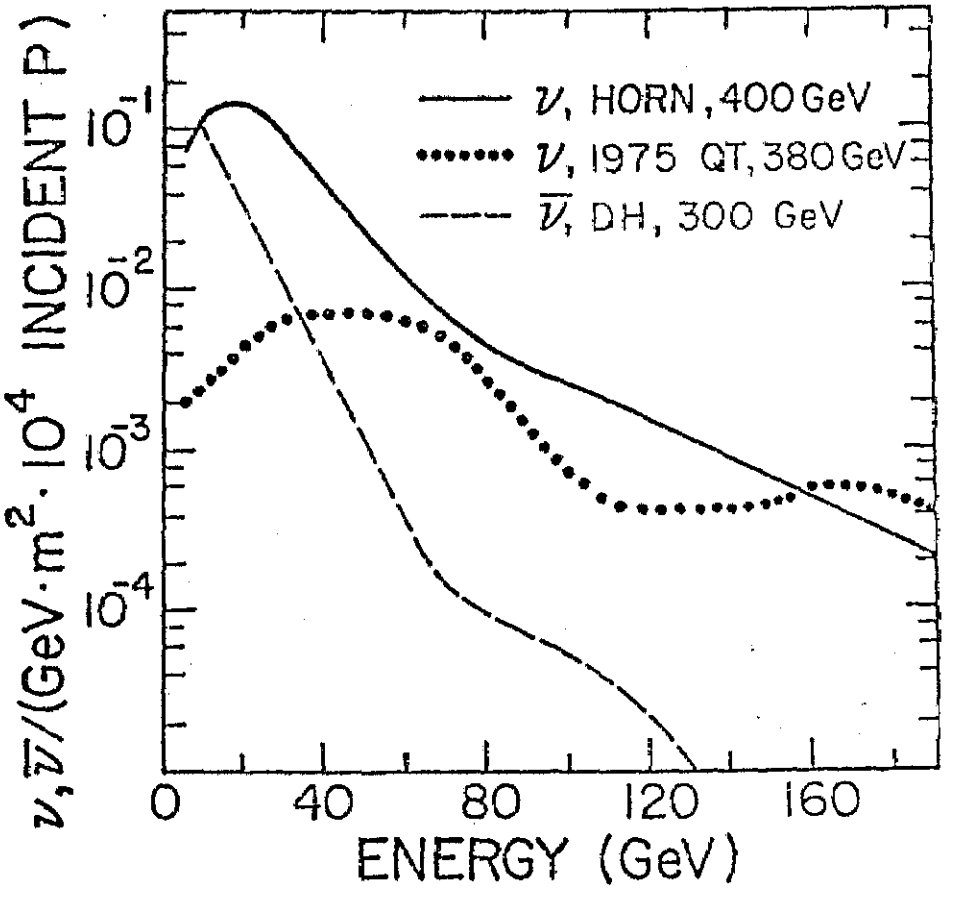

FIGURE 4

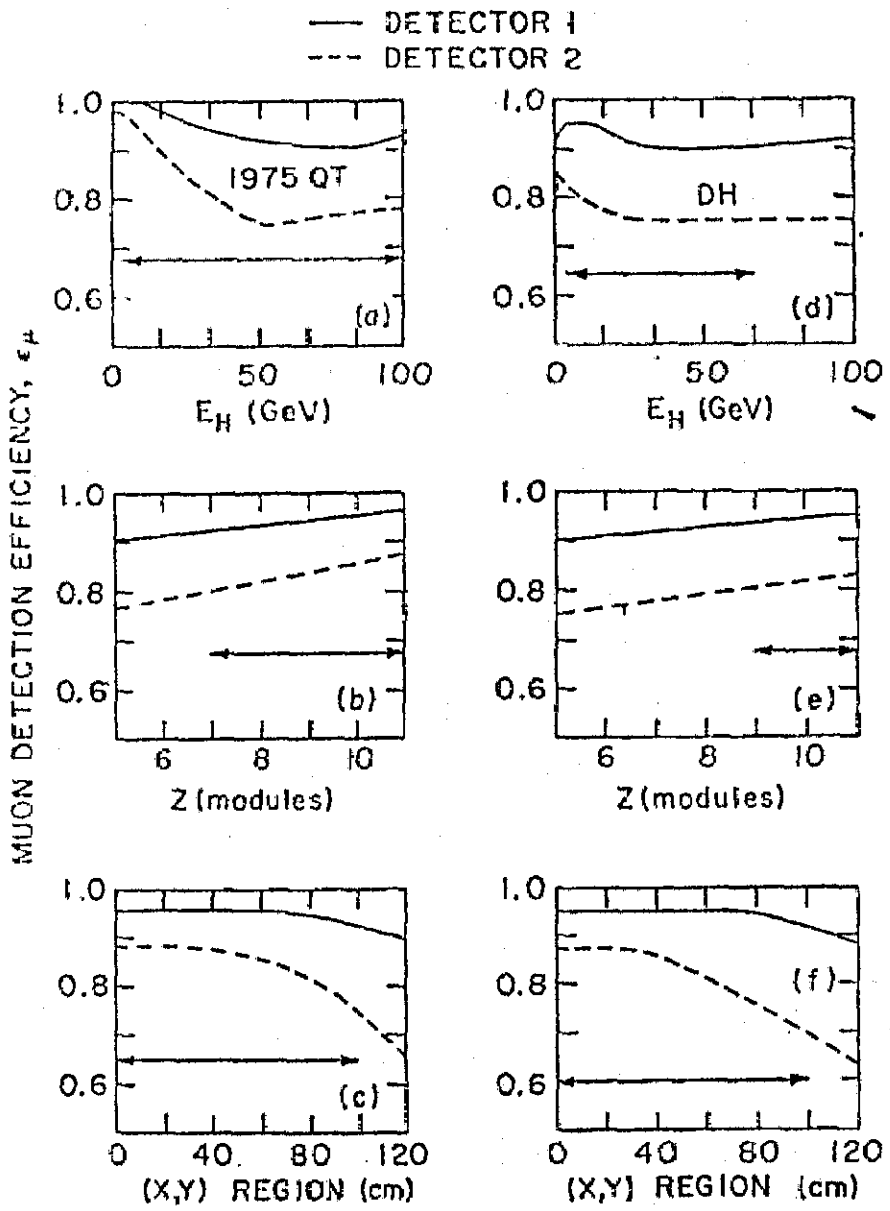

FIGURE 5

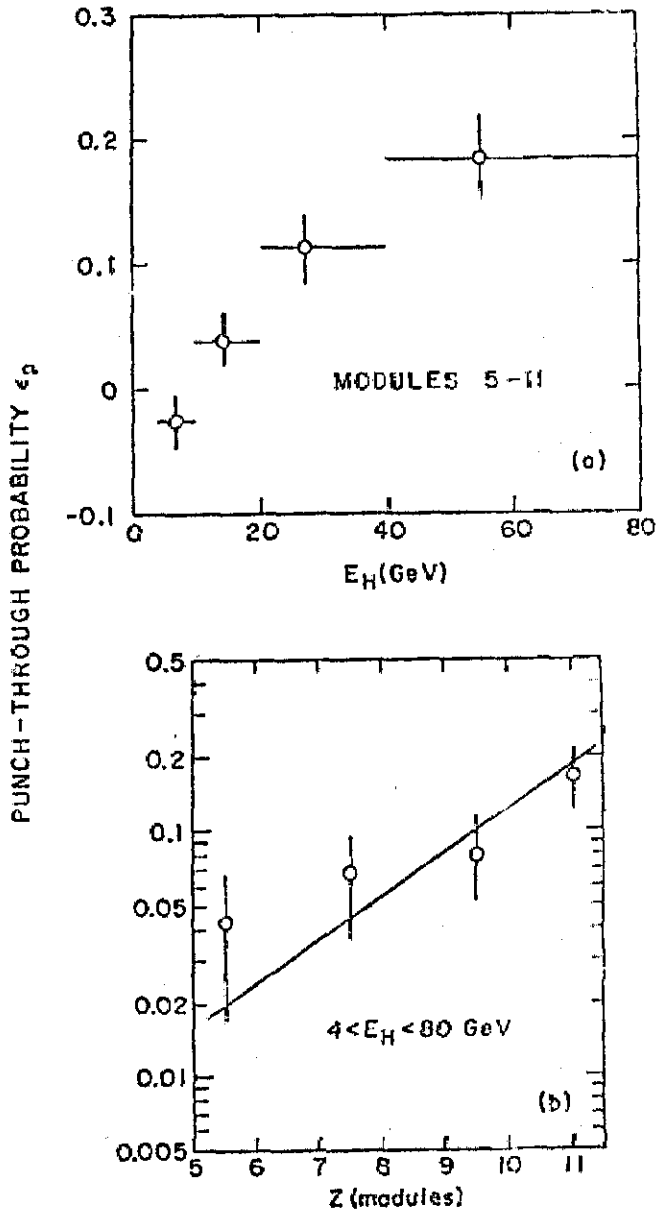

FIGURE 6

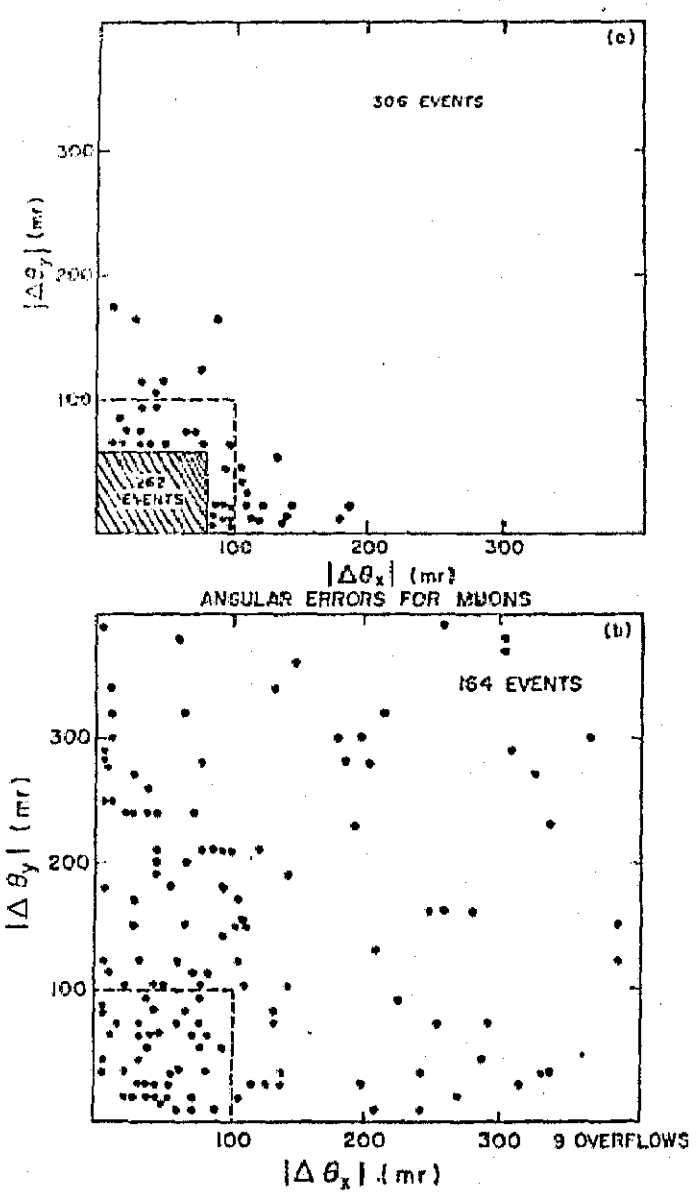

FIGURE 7

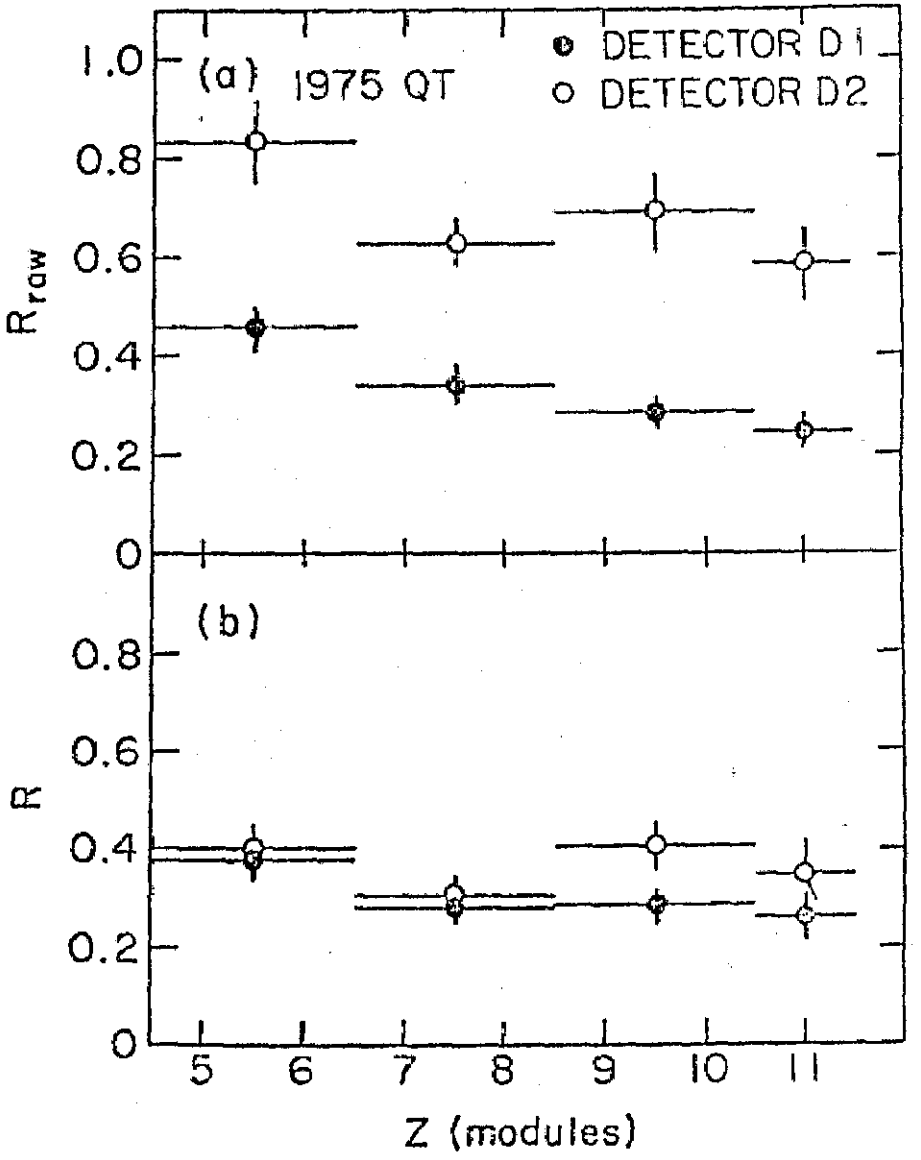

FIGURE 8

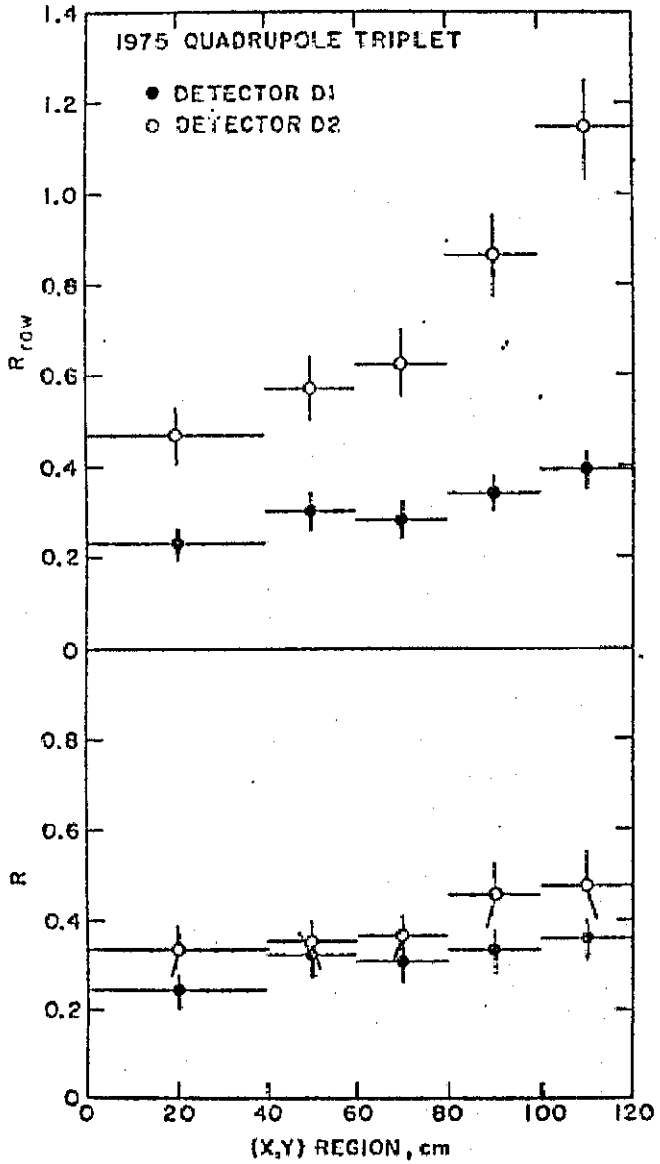

FIGURE 9

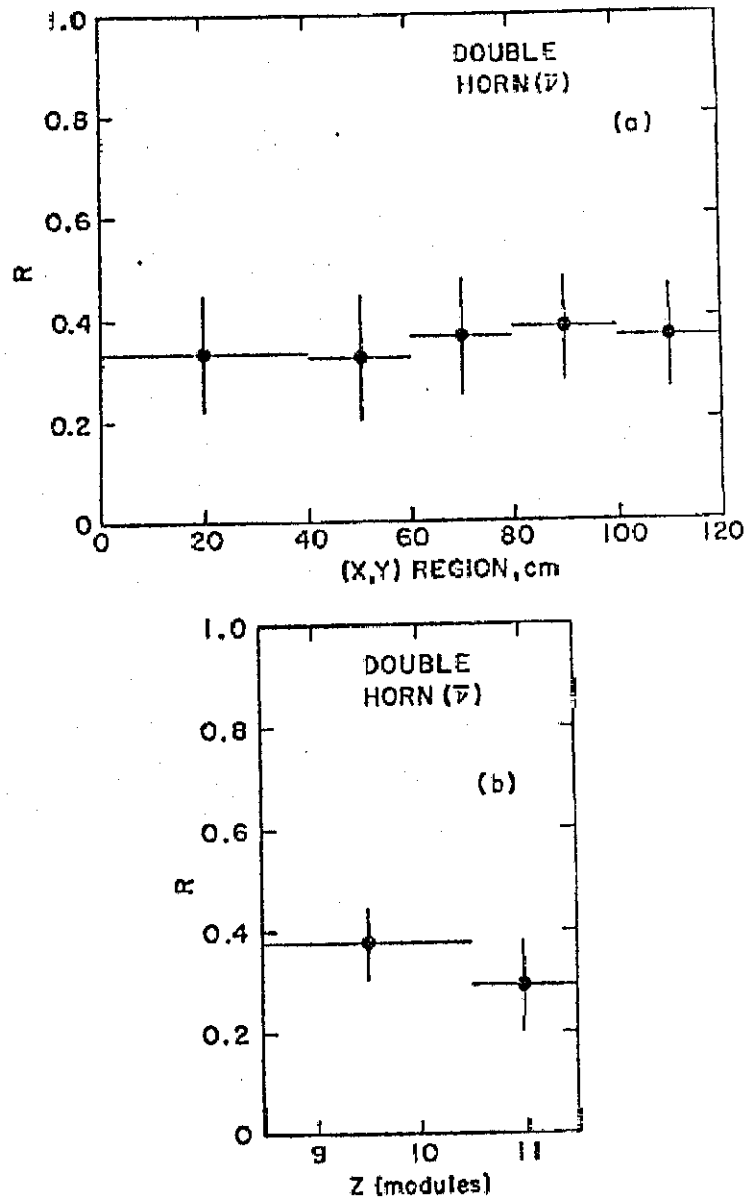

FIGURE 10

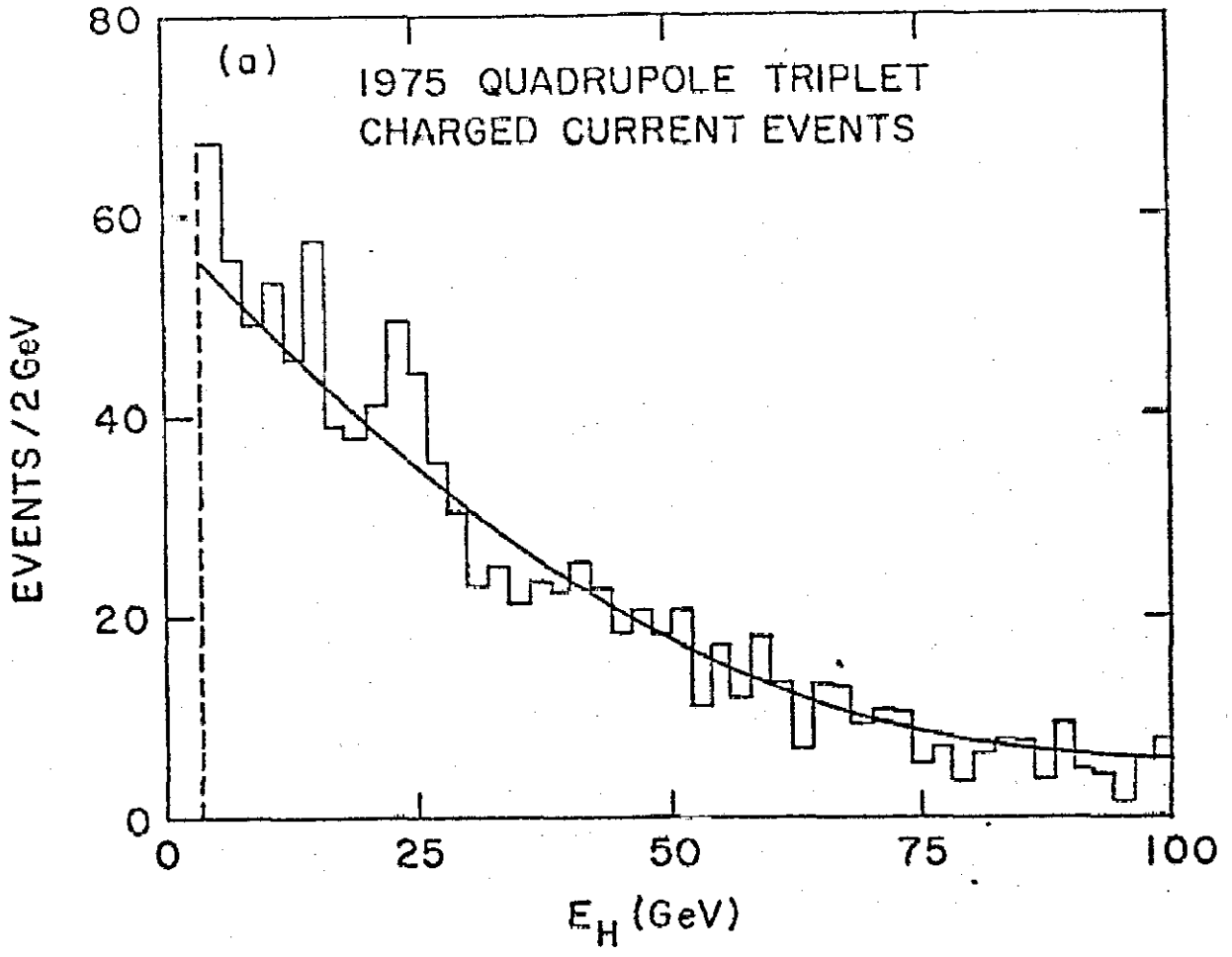
(a)
1975 QUADRUPOLE TRIPLET
CHARGED CURRENT EVENTS
EVENTS / 2 GeV
80
60
40
20
0
0
25
50
75
100
E_H (GeV)

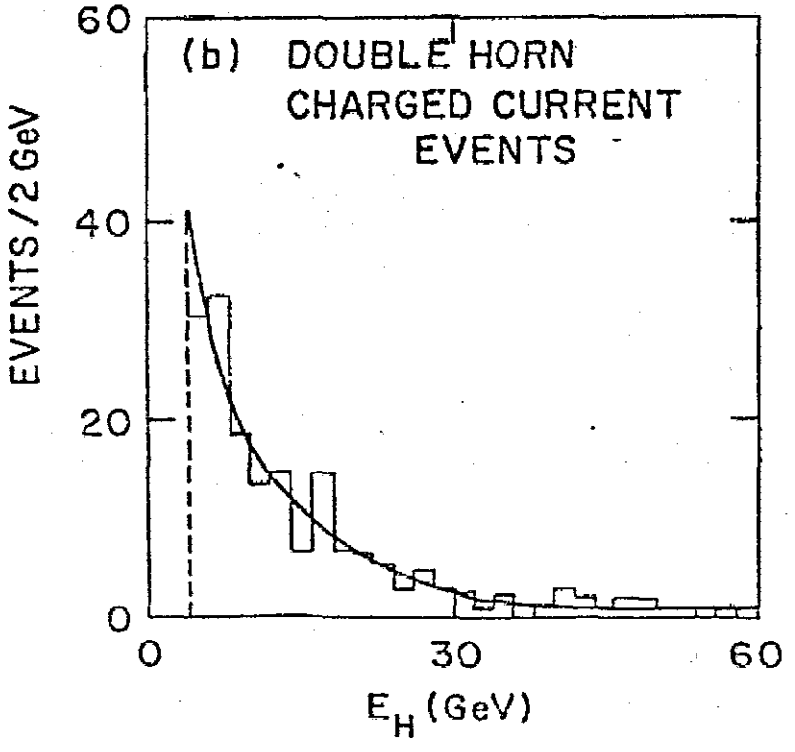
(b) DOUBLE HORN
CHARGED CURRENT
EVENTS
EVENTS / 2 GeV
60
40
20
0
0
30
60
E_H (GeV)

FIGURE 11

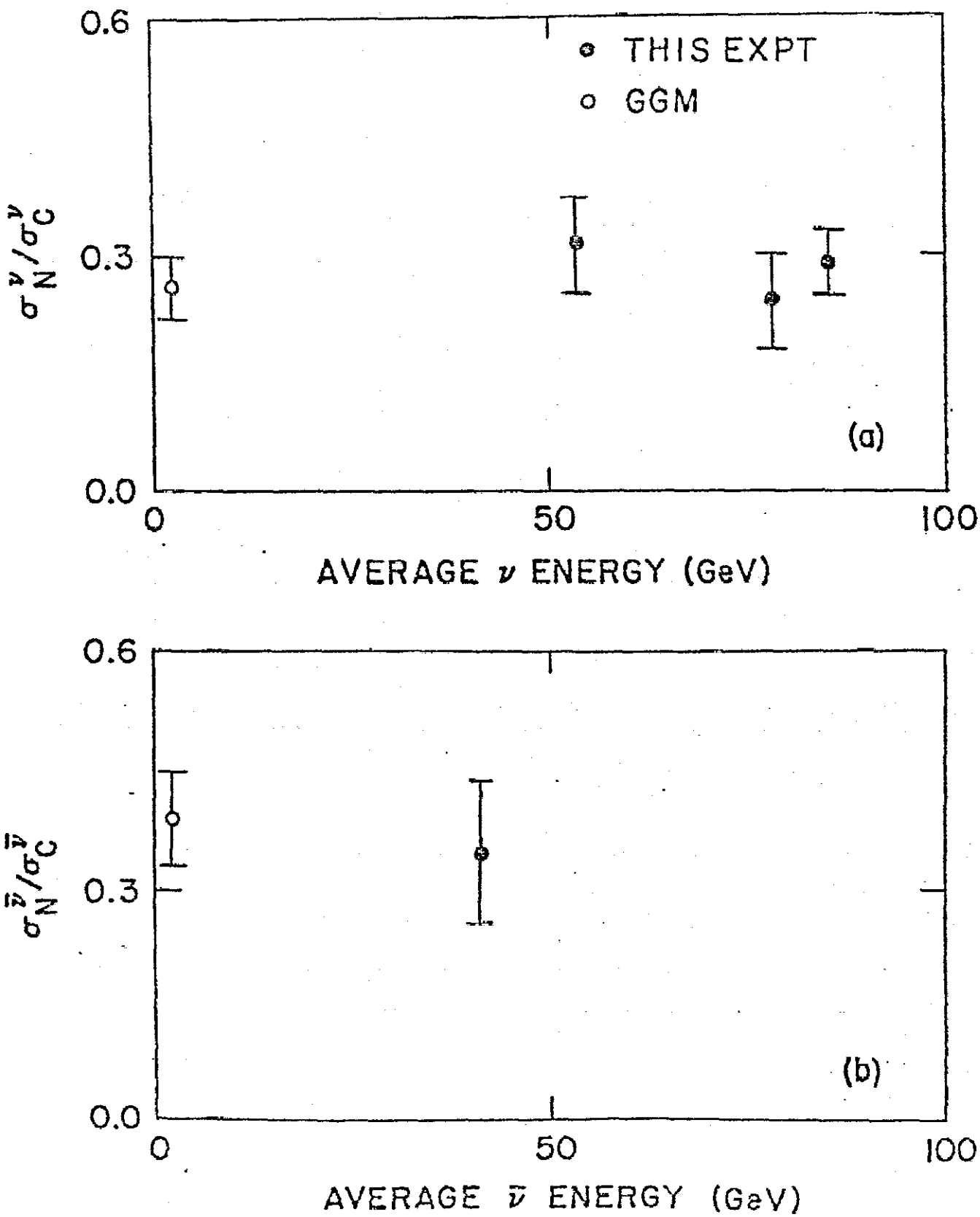
0.6
0.3
0.0
$\sigma_N^{\nu}/\sigma_C^{\nu}$
THIS EXPT
GGM
(a)
0
50
100
AVERAGE ν ENERGY (GeV)
0.6
0.3
0.0
$\sigma_N^{\bar{\nu}}/\sigma_C^{\bar{\nu}}$
(b)
0
50
100
AVERAGE $\bar{\nu}$ ENERGY (GeV)

FIGURE 12

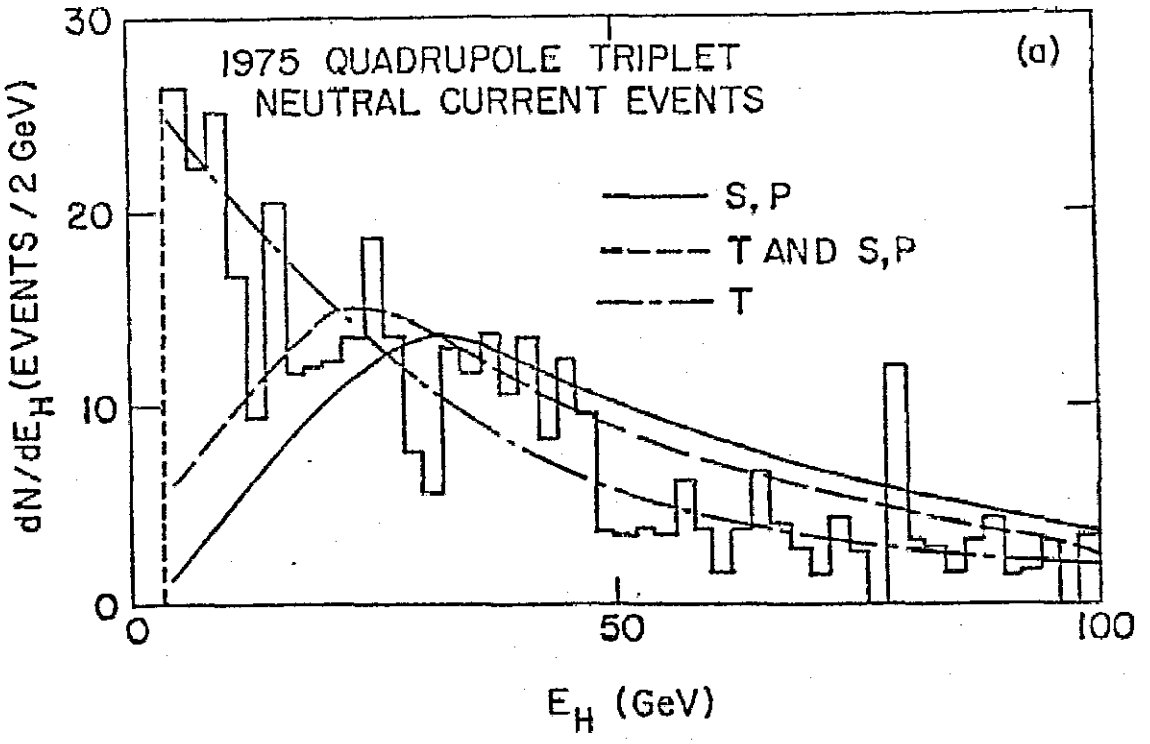
1975 QUADRUPOLE TRIPLET
NEUTRAL CURRENT EVENTS
(a)
S, P
T AND S,P
T
dN/dE_H (EVENTS / 2 GeV)
E_H (GeV)
0
10
20
30
0
50
100

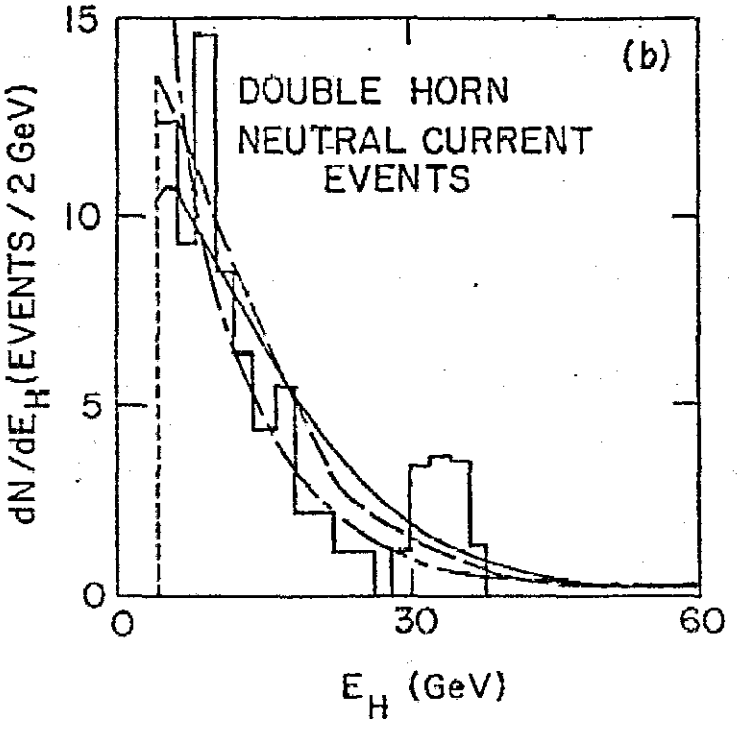
DOUBLE HORN
NEUTRAL CURRENT
EVENTS
(b)
dN/dE_H (EVENTS / 2 GeV)
E_H (GeV)
0
5
10
15
0
30
60

FIGURE 13

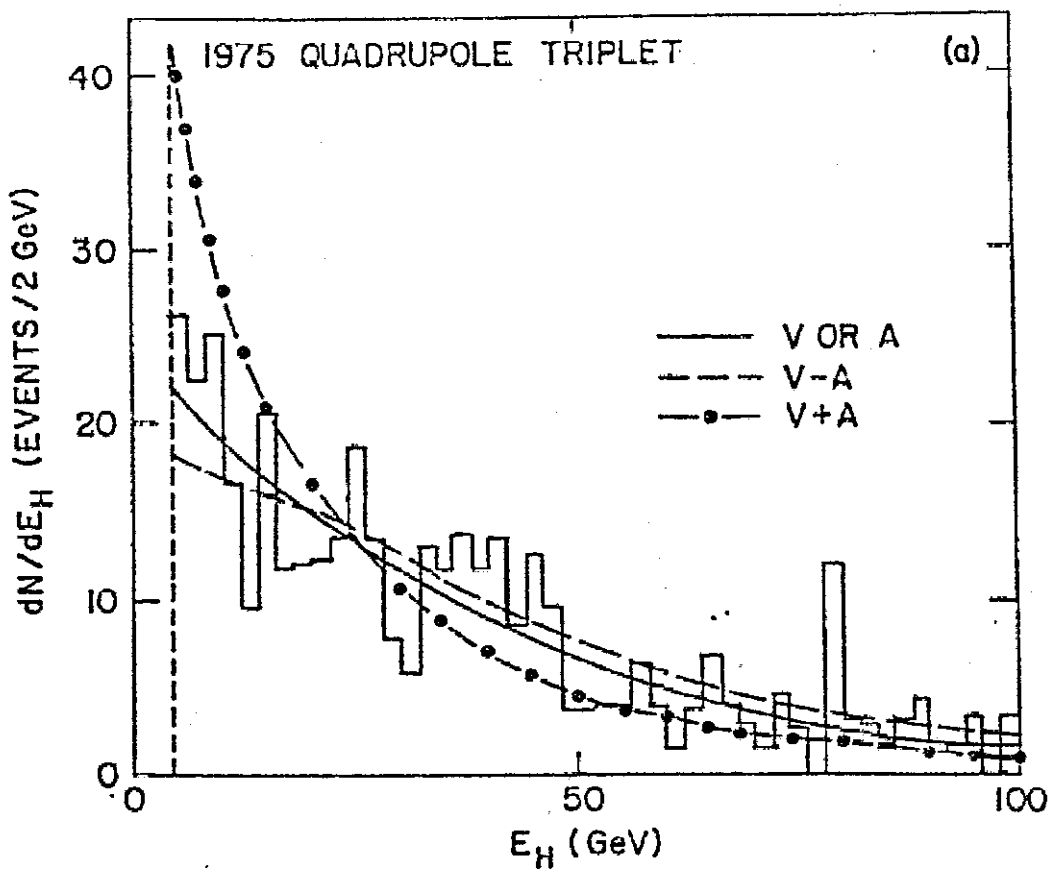
1975 QUADRUPOLE TRIPLET
(a)
V OR A
V-A
V+A
dN/dE_H (EVENTS/2 GeV)
E_H (GeV)
0
10
20
30
40
50
100

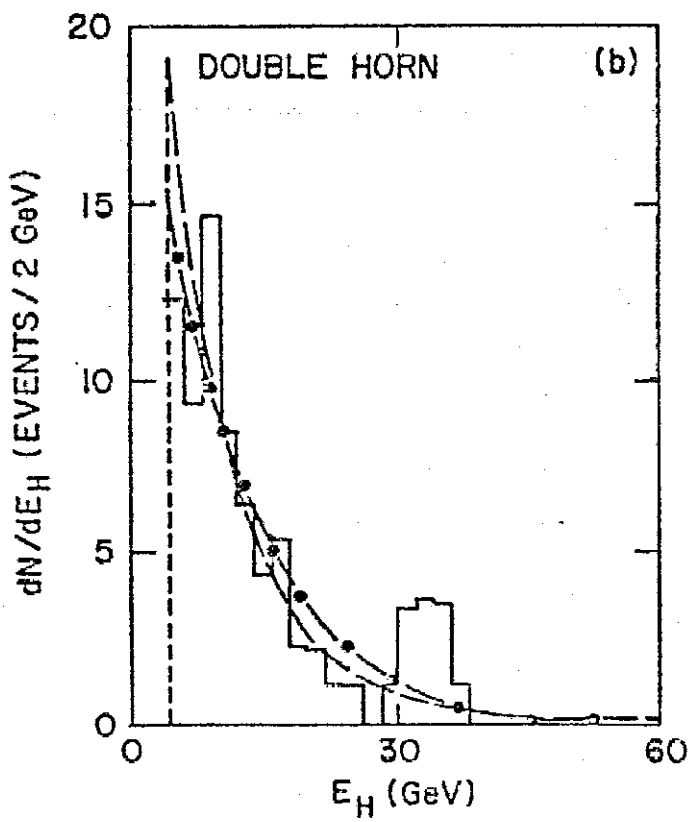
DOUBLE HORN
(b)
dN/dE_H (EVENTS/2 GeV)
E_H (GeV)
0
5
10
15
20
30
60

FIGURE 14

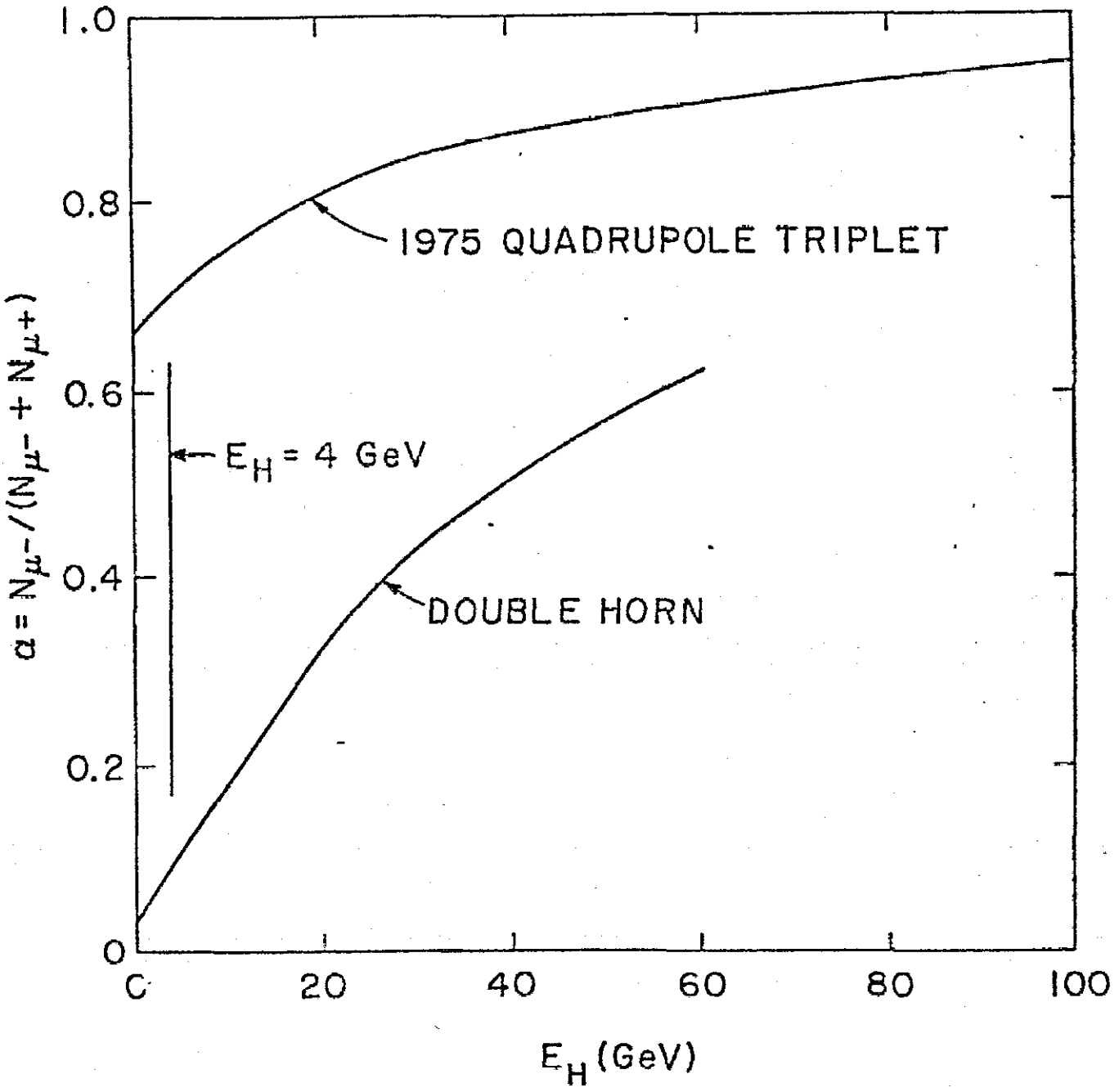
1.0
0.8
0.6
0.4
0.2
0
$\alpha = N_{\mu^-}/(N_{\mu^-} + N_{\mu^+})$
1975 QUADRUPOLE TRIPLET
E_H = 4 GeV
DOUBLE HORN
0
20
40
60
80
100
E_H (GeV)

FIGURE 15

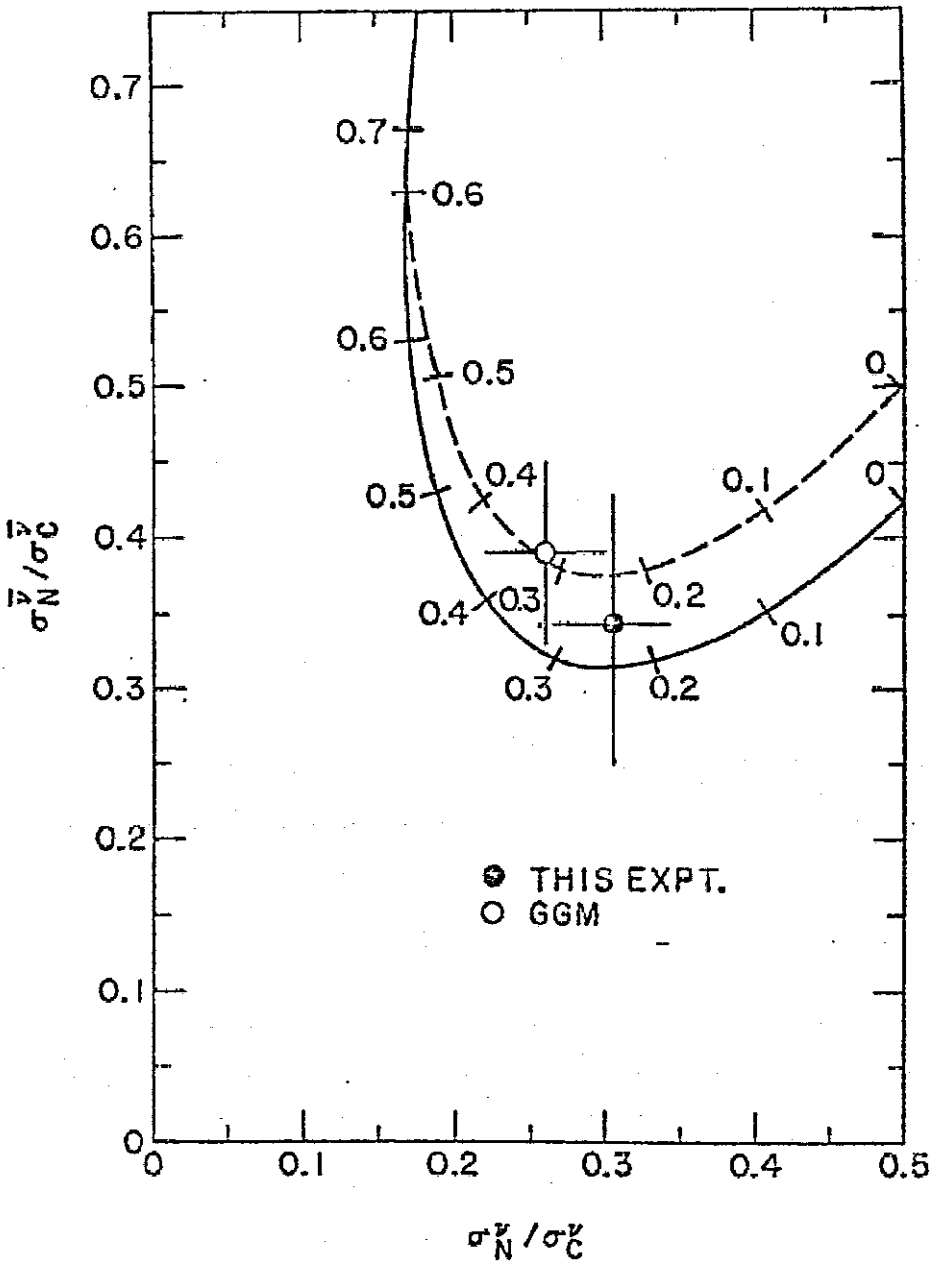
0.7
0.6
0.5
0.4
0.3
0.2
0.1
0
0.1
0.2
0.3
0.4
0.5
$\sigma_N^{\bar{\nu}}/\sigma_C^{\bar{\nu}}$
$\sigma_N^{\nu}/\sigma_C^{\nu}$
THIS EXPT.
GGM

FIGURE 16

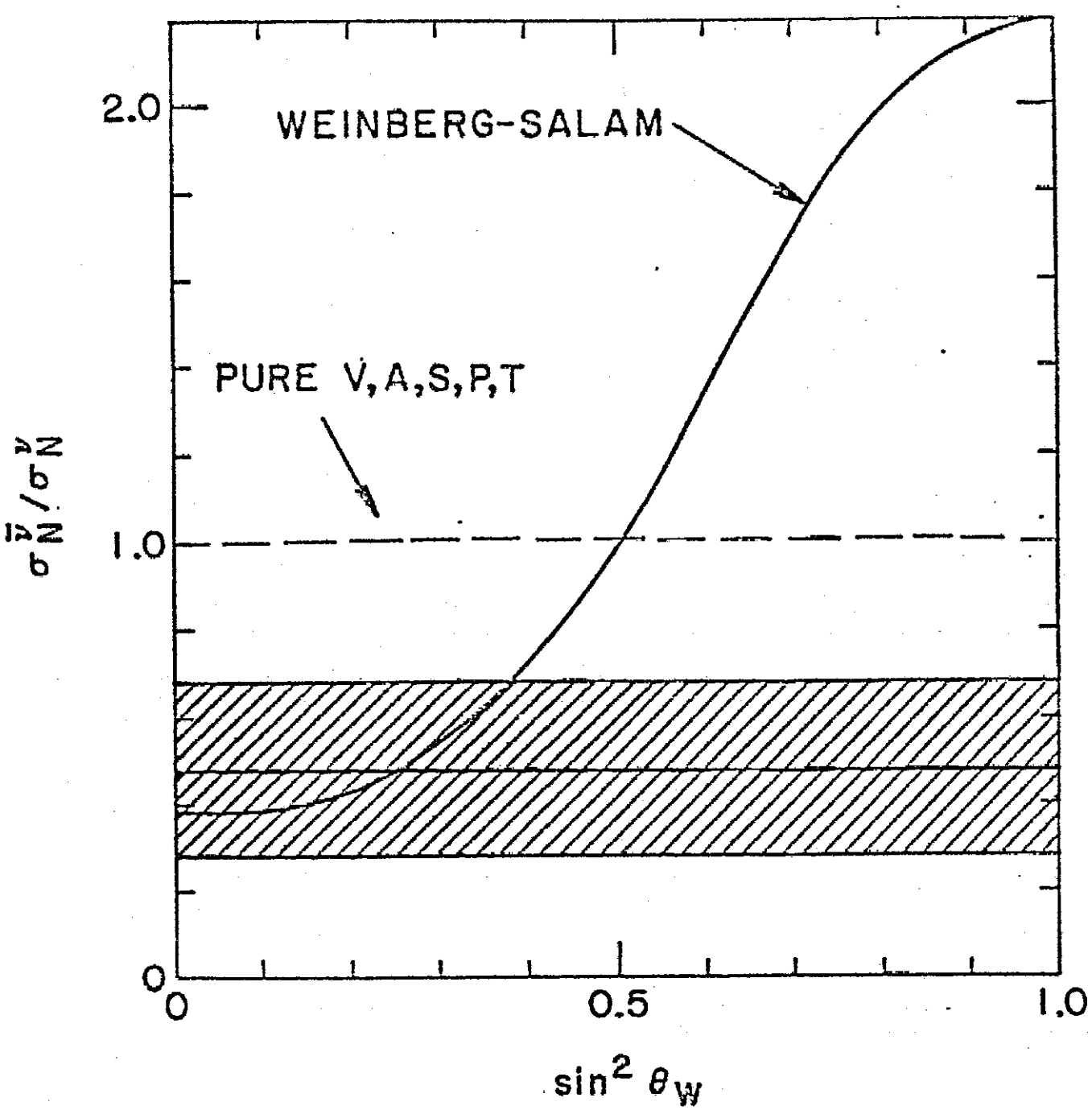
2.0
1.0
0
WEINBERG-SALAM
PURE V,A,S,P,T
$\sigma_N^{\bar{\nu}}/\sigma_N^{\nu}$
0
0.5
1.0
$\sin^2\theta_W$

FIGURE 17